

1995

The ultrasonographic differentiation of obstructive vs. nonobstructive hydronephrosis in children

Barbara Marie García
Yale University

Follow this and additional works at: <http://elischolar.library.yale.edu/ymtdl>

Recommended Citation

García, Barbara Marie, "The ultrasonographic differentiation of obstructive vs. nonobstructive hydronephrosis in children" (1995).
Yale Medicine Thesis Digital Library. 2626.
<http://elischolar.library.yale.edu/ymtdl/2626>

This Open Access Thesis is brought to you for free and open access by the School of Medicine at EliScholar – A Digital Platform for Scholarly Publishing at Yale. It has been accepted for inclusion in Yale Medicine Thesis Digital Library by an authorized administrator of EliScholar – A Digital Platform for Scholarly Publishing at Yale. For more information, please contact elischolar@yale.edu.

YALE UNIVERSITY LIBRARY



39002086760171

THE ULTRASONOGRAPHIC
DIFFERENTIATION OF OBSTRUCTIVE VS.
NONOBSTRUCTIVE HYDRONEPHROSIS
IN CHILDREN: A MULTIVARIATE
SCORING SYSTEM



Barbara Marie Garcia


1995

YALE
UNIVERSITY




CUSHING/WHITNEY
MEDICAL LIBRARY

Permission to photocopy or microfilm processing of this thesis for the purpose of individual scholarly consultation or reference is hereby granted by the author. This permission is not to be interpreted as affecting publication of this work or otherwise placing it in the public domain, and the author reserves all rights of ownership guaranteed under common law protection of unpublished manuscripts.


Signature of Author

5/8 /95
Date



Digitized by the Internet Archive
in 2017 with funding from
The National Endowment for the Humanities and the Arcadia Fund

<https://archive.org/details/ultrasonographic00garc>

**THE ULTRASONOGRAPHIC DIFFERENTIATION OF
OBSTRUCTIVE VS. NONOBSTRUCTIVE HYDRONEPHROSIS IN
CHILDREN: A MULTIVARIATE SCORING SYSTEM**

**A Thesis Submitted to the
Yale University School of Medicine
in Partial Fulfillment of
the Requirements for the
Degree of Doctor of Medicine**

**by
Barbara Marie García
1995**

YALE MEDICAL LIBRARY

OCT 12 1995

Med Lib

T113

+Y12

6292

DEDICATION

This thesis is dedicated to my grandmother, Baba, who through her upbringing, taught me what is truly important in this world. Her sacrifices, wisdom, and genuine love, I shall always cherish for the remainder of my life. Te extraño, Baba.

ACKNOWLEDGMENTS

I feel very fortunate to have had Dr. Marc Keller as my advisor. Through his commitment and dedication, he has taught me much about how to design and perform clinical research . His constructive input during the writing of my thesis was instrumental and very much appreciated. I would also like to thank the Department of Diagnostic Radiology for providing me with the resources and advisors to pursue this worthwhile project.

I would like to thank Dr. Holly Korsvik , Dr. Dana Schwartz as well as Dr. Marc Keller, for performing all of the renal ultrasounds and for obtaining the beautiful photographs that were used in this study. Thanks to Lisa Varipapa for helping me with graphics and for allowing me to take over her desk from time to time. Thanks also to Dr. Robert Weiss, who was instrumental in providing all of the subjects for this work.

Special thanks to the Office for Student Research and Dr. John Forrest who made this learning experience come to fruition.

I shall end by especially thanking my mother, father, brother and grandmother for all of their love and support, not only during the writing of this thesis, but throughout my hectic life. Thanks to my beloved Tino, for helping me with my computer illiteracy, and more importantly, for his continual support and encouragement in every aspect of my life. One last heartfelt thank you to God, for granting me the opportunity to attend Yale and to learn about the exciting and ever-changing field that is called medicine.

TABLE OF CONTENTS

	Page
ABSTRACT.....	1
INTRODUCTION.....	3
PART I -----	
ANATOMY OF THE URINARY SYSTEM.....	5
EMBRYOLOGY OF THE URINARY SYSTEM.....	6
PHYSIOLOGY OF THE URINARY SYSTEM.....	8
PART II -----	
URINARY TRACT OBSTRUCTION.....	11
ETIOLOGIES OF URINARY TRACT OBSTRUCTION IN THE PEDIATRIC POPULATION.....	14
OTHER CAUSES OF HYDRONEPHROSIS.....	17
PART III -----	
HISTORY OF DIAGNOSTIC ULTRASOUND.....	20
PHYSICS OF DIAGNOSTIC ULTRASOUND.....	25
DOPPLER ULTRASOUND.....	34
PART IV -----	
PRENATAL SCREENING OF HYDRONEPHROSIS.....	40
DIAGNOSIS OF URINARY TRACT OBSTRUCTION IN THE PEDIATRIC POPULATION.....	42
DIAGNOSIS OF URINARY TRACT OBSTRUCTION BY SONOGRAPHY IN THE PEDIATRIC PATIENT.....	50
PURPOSE.....	69
MATERIALS AND METHODS.....	70
RESULTS.....	79
DISCUSSION.....	90
CONCLUSION.....	95
REFERENCES.....	96

ABSTRACT

THE ULTRASONOGRAPHIC DIFFERENTIATION OF OBSTRUCTIVE VS. NON-OBSTRUCTIVE HYDRONEPHROSIS IN CHILDREN: A MULTIVARIATE SCORING SYSTEM. Barbara M. García and Marc S. Keller. Section of Pediatric Diagnostic Imaging, Department of Diagnostic Radiology, Yale University School of Medicine, New Haven, CT.

The purpose of this study was to identify sonographic prognosticators to aid in distinguishing obstructive from nonobstructive hydronephrosis in children and to develop a scoring system using these indicators in order to predict the risk of a child having urinary tract obstruction.

The sonographic and radiologic reports of 635 kidneys and collecting systems in 320 children were retrospectively reviewed. Twelve sonographic variables were initially analyzed to determine significant association between the variables and the presence of urinary tract obstruction. The significant findings were subsequently subjected to logistic regression models to identify potential predictors for obstructive hydronephrosis.

Ten variables were found to be significantly associated with urinary tract obstruction in the preliminary univariate analyses. After being subjected to logistic regression, seven variables were determined to be associated with a significantly higher risk of urinary tract obstruction. These variables were utilized for the development of the hydronephrosis obstructive multivariate scoring system. Patients were subsequently assigned to high, intermediate and low risk groups according to their obstructive scores,

with a predicted probability of having urinary tract obstruction for each group of approximately $\leq 30\%$, 31-67% and $\geq 68\%$, respectively. The probability of possessing urinary tract obstruction increased with higher obstructive scores. High scores on the scoring system had a sensitivity of detecting obstruction of 91% and a false positive rate of 1.0%. Low scores excluded obstruction with a specificity of 99% and a false negative rate of 9.0%. The accuracy of the obstructive scoring system was 97.9%.

The obstructive scoring system shows promise as a method for the differentiation of obstructive from nonobstructive hydronephrosis in children and may, in the future, obviate the need for other more invasive, radiation-exposing, and more expensive examinations in this population.

INTRODUCTION

The primary goal of the urologist is the preservation of the kidney and its function. This is especially true when the patients involved are children, in whom growth and development of the kidneys and urinary tract is still in progress. Failure to recognize and treat serious pathology in the pediatric urinary tract may result in the unfortunate demise of the involved kidney and loss of function. To better understand the malformations and pathology which may lead to such consequences in children, knowledge of the anatomy, embryology and physiology of the individual organs of the complete urinary system is needed. This work shall begin with a brief summary of the aforementioned topics, followed by a description of the causes and significance of urinary tract obstruction and hydronephrosis in children.

The diagnosis of hydronephrosis and urinary tract obstruction in children depend strongly upon diagnostic radiology. The radiologist relies upon several methods of diagnostic imaging, including one of the newer modalities in radiology and the diagnostic tool upon which the focus of this work is placed, ultrasonography. To understand the strengths, limitations, and importance of this imaging technique, one should be familiar with the intriguing history and physical principles which underlie it. This shall be the focus of the third section of this introduction.

Presently, the major role of diagnostic ultrasound in pediatric hydronephrosis lies in the screening and detection of collecting system dilatation with the actual diagnosis of the underlying etiology confirmed by other diagnostic imaging modalities. However, in recent years, several investigations have emerged regarding the utility of diagnostic ultrasound in the diagnosis of urinary tract obstruction, and consequently, this has

sparked intense interest in both pediatric sonographers and urologists alike to further investigate the effectiveness and reliability of ultrasound as a primary diagnostic tool. The fourth section of the introduction focuses on the usefulness of diagnostic ultrasonography in the screening of hydronephrosis in the prenatal period as well as the current methods of imaging the kidneys and the urinary system in children for the diagnosis of urinary tract obstruction. Finally, this introduction shall conclude with the recent work that has been published regarding the specific use of ultrasonography in the differentiation of obstructive from nonobstructive hydronephrosis, particularly in regard to the pediatric population.

PART I

ANATOMY OF THE URINARY SYSTEM

The kidneys are retroperitoneal organs which lie on the posterior abdominal wall. These bean-shaped organs lie alongside the upper lumbar vertebrae, anterior to the psoas major muscles (1). In approximately 90% of individuals, the left kidney is found one to two centimeters higher than the right, owing to the large right lobe of the liver (2). The upper portions of the kidneys are encased by the bony thorax and are tilted so that the superior poles are located more medially than the inferior poles. Adult human kidneys measure approximately 10 cm in length, 5 cm in width and 2.5 cm in thickness (3). However, the size of pediatric kidneys are age-dependent. Each kidney has a concave, central portion termed the hilum, through which pass the renal artery, vein, nerves and lymphatics. The hilum leads into a space within the kidney called the renal sinus (1). The renal sinus contains the renal pelvis, which is the superior expanded end of the ureter. The pelvis divides into two or sometimes three, wide tube-like funnels called the major calyces. Each of the major calyces are divided into seven to fourteen minor calyces (4). The urine flows from the glomerulus, the proximal tubule, the loop of Henle, and the distal tubule through the collecting ducts into the minor calyces via openings in the renal papillae. From the minor calyces, the urine then passes into the major calyces, the renal pelvis and subsequently, into the ureters (2).

Each kidney has originating from its pelvis, a ureter, which is an expansile, thick-walled, muscular duct that extends to the urinary bladder. Throughout its entire length, the ureter is retroperitoneal. It descends longitudinally along the psoas major muscle, crosses the pelvic brim and external iliac artery, and enters the base of the bladder at the lateral margins of the trigone (ureterovesical junction) (5). The diameter of the ureter

varies widely, having an average width of 5mm, with the narrowest portions found at the ureteropelvic junction, at the crossing of the external iliac artery and at the entrance into the bladder. However, the ureters are dynamic organs with diameters that are constantly changing due to peristalsis (6).

Both ureters enter the bladder obliquely at its base, where they define two angles of the trigone, a triangular area with a smooth surface. The position of the bladder, the urinary reservoir, is in the pelvis for adults, just below the inferior peritoneal reflection (6). Interestingly, in infants and young children, the urinary bladder is located in the abdomen, even when empty. The bladder begins to enter the pelvis at about six years of age (7). It is an organ which varies greatly in contour and size depending upon the amount of filling. The normal capacity of the adult bladder can vary between 300 to 1000 ml.

The female urethra is a short, straight muscular tube which is about 3-4 cm in length. It defines the third angle of the bladder trigone, passes anteroinferiorly from the urinary bladder and ends between the labia minora, just anterior to the vaginal orifice. In the male, the urethra is divided into three parts: the prostatic urethra, the membranous urethra and the spongy, or anterior, urethra. It courses from the urinary bladder to the external urethral orifice found at the tip of the glans penis (7).

EMBRYOLOGY OF THE URINARY SYSTEM

The origin of the kidney is from the nephrogenic mesoderm, which is derived from the intermediate mesoderm (1). Three different sets of "kidneys" have been shown to develop in the human embryo: the pronephros, the mesonephros and the metanephros.

The pronephros develop early during the fourth week of gestation and are completely nonfunctional. These primitive kidneys are succeeded by the mesonephros, which appear caudal to the pronephros later in the fourth week of embryonic life. The mesonephric kidneys contain glomeruli and tubules and are thereby functional. The metanephros, the permanent kidneys, develop early in the fifth week and are functional approximately six weeks later (2).

At 13 weeks, the ureter begins to appear as a metanephric duct (dorsal bud) which arises from the mesonephric duct, which is ultimately an extension of a duct from the pronephros. This ureteric bud grows and subsequently connects to undifferentiated mesenchyme, which lies caudal to the mesonephros and thus, the ureteropelvic junction is formed. By approximately 21 weeks gestation, the ureteric bud begins to branch to form secondary buds. The stalk of the bud becomes the ureter and its funnel-shaped cranial end becomes the renal pelvis. The first four generations of buds eventually become the major calyces and the second four generations evolve into the minor calyces (3). Further branching of the ureteric bud forms the collecting ducts. The end of each of these collecting tubules subsequently induces cells in the mesenchyme of the metanephric mesoderm to develop into small metanephric vesicles. These vesicles eventually differentiate into the nephron, which then connects with the collecting tubules which arose from the ureteral bud (1).

Once the kidney has been formed, its ascent commences. Initially, the kidneys lie side by side in the pelvis. As the abdomen lengthens, the kidneys slowly move further apart and come to lie in the abdomen (2). The kidney reaches the level of the third lumbar vertebrae at the end of the third month of gestation. During the ascent, the hilum of the kidney, which originally faced ventrally, rotates medially 90 degrees to terminate in its anteromedial adult position (2).

The fetal kidneys are divided into lobes that are potentially visible on their surfaces as elevations. These lobes are the functional parenchymal units of the kidney which develop at the same time as the minor calyces. The lobulation usually disappears during infancy as the nephrons mature and develop (1).

During the fifth week of gestation, cloacal division commences. The anterior portion of the cloaca becomes the urogenital sinus and the posterior aspect, the rectum (4). The urogenital sinus subsequently develops into the superiorly located vesicourethral canal, which gives rise to the bladder and upper urethra, and the inferiorly located definitive urogenital sinus, from which the main portion of the urethra is formed. By the fourth month of gestation, the vesicourethral canal has enlarged and developed into the fully-formed urinary bladder (1).

The epithelium of the entire female urethra and the posterior male urethra is derived from the endoderm of the distal portion of the urogenital sinus. The remainder of the male urethra develops from the definitive urogenital sinus. The prostate subsequently develops by budding from the formed posterior urethra (4).

PHYSIOLOGY OF THE URINARY SYSTEM

The kidneys are regulatory organs that control the excretion of water and a variety of dissolved substances and thus, help maintain a constant and optimal internal environment. In addition to stabilizing the total solute concentration of body fluids, the kidney also regulates the circulating concentrations of individual solutes such as sodium,

potassium, hydrogen ion, calcium, chloride, bicarbonate, phosphate, sulfate, glucose, urea, creatinine, amino acids and uric acid (1).

The glomerular filtrate is a protein-free solution that is initially separated from plasma. The blood flow to the kidneys is quite voluminous, approximately 20% of the cardiac output, which results in a renal blood flow of 1250 ml per minute (2). In the adult, the glomerular filtration rate is approximately 125 ml per minute, which is subsequently reduced by reabsorption from the proximal tubule to the normal urine output of 1 ml per minute. The filtrate then passes to the loop of Henle where the countercurrent exchange system creates a high concentration of solute in the medulla due to the active transport of sodium from the ascending limb of the loop of Henle. This results in a high osmotic gradient between the collecting ducts and the medulla which gradually allows water to flow from the collecting ducts into the medulla and consequently results in a concentrated urine (3).

By varying the rate of bicarbonate and acid secretion, the kidney functions as an important regulator of acid-base balance. Another major regulatory function of the kidney is acting as an endocrine organ by producing and releasing several hormones, such as renin, kallikrein, erythropoietin, $1, 25 (\text{OH})_2 \text{D}_3$, eicosanoids and dopamine (4).

After the urine is formed by the kidney, it is transported to the bladder by the collecting systems and ureters. Each calyx functions asynchronously and independently in delivering urine to the renal pelvis. Once urine distends the pelvis, the first propagating wave of peristalsis commences in the pelviureteric region. The wave then is transmitted down the ureter via an electrical impulse that passes consecutively through smooth muscle cells in the ureteral wall (5). As the superior segment of the ureter contracts to propel the urine towards the bladder, the segment directly below relaxes to accept the

bolus. This sequence of contraction and relaxation repeats itself until the urine reaches the bladder (3). The rate of these peristaltic waves is approximately one to five per minute. The ureters pass obliquely through the bladder wall and this geometric positioning tends to keep the ureterovesical junctions closed (except during the peristaltic waves) and thus, prevents reflux of urine from the bladder (4).

The reflex arc in micturition depends upon the parasympathetic system and is derived from the second through the fourth sacral cord segments. However, the external urethral sphincter has its innervation from the somatic system. In response to bladder distention, receptors within its wall initiate the micturition reflex. The voiding reflex can subsequently be facilitated or inhibited by the cerebral cortex (3). During the process of voiding, the detrusor muscle contracts, the perineal muscles and external urethral sphincter relax and the urine passes out through the urethra. Urinary continence is maintained by the internal and external sphincters combined (4).

PART II

URINARY TRACT OBSTRUCTION

Obstruction to the passage of urine can occur anywhere along the urinary tract, from the level of the renal tubules to the external urethral meatus (1). Urinary tract obstruction can be unilateral or bilateral, partial or complete, sudden or chronic. It can be caused by extrinsic processes that compress the ureter or from lesions that are intrinsic to the urinary tract (2). In addition, cases of urinary tract obstruction can exhibit tremendous variety with regard to severity, duration, rapidity of onset and persistence of residual abnormalities (3).

Unrelieved urinary tract obstruction has been shown to interfere with normal development of the kidney in young children and almost always leads to permanent renal atrophy, termed obstructive uropathy (2). Furthermore, the severity of the obstructive uropathy depends on the duration and degree of obstruction present (4). Fortunately, most etiologies of urinary tract obstruction are surgically correctable or can be treated medically (2). However, the earlier urinary obstruction is diagnosed, especially in regard to children, the better prognosis for retainment or recovery of full renal function.

When ureteral obstruction is complete, a rise in urine pressure proximal to the site of obstruction is found, which is proportional to the degree of obstruction present. This causes a dilatation of the renal pelvis and calyces, termed hydronephrosis, and associated dilatation of the proximal ureter, termed hydroureter, associated with progressive atrophy of the kidney. Obviously, it is not the dilatation of the ureter that is of significance in cases of obstruction, but the consequent involvement of the kidneys (5). Increased pressure in the calyces causes a well-known series of events within the kidney. Filtration in the glomerulus persists for a period of time as the pressure in the tubular lumina rises,

because the filtrate diffuses into the renal interstitium where it subsequently returns to the lymphatic and venous systems (2,3). Because of the continued filtration, the calyces and pelvis become dilated. Consequently, pressure in the Bowman's capsule rises and the glomerular filtration rate begins to decrease (6). If the pressure remains elevated in Bowman's capsule, the blood flow to the affected kidney will begin to decrease and in turn, the rate of flow of the filtrate in the tubules decreases, as well as the ability of the kidney to concentrate urine. If the obstruction persists, the changes in the renal cortex progress. Renal blood flow continues to fall and the glomerular filtration rate drops further and may even disappear. Ultimately, the volume of the cortex begins to diminish as the cells of the tubules atrophy (7). In addition, this high pressure also compresses the renal vasculature of the medulla, causing a decrease in inner medullary plasma flow. Thus, if the obstruction is protracted, medullary functional disturbances will ensue and chronic renal failure may result (2).

Normal peristalsis of the ureters is impaired by the elevated pressure in the collecting system. The ureters become distended and the waves of peristalsis become ineffective, no longer being able to completely close the ureteral lumen, or peristalsis may even cease altogether. The ureter and its collecting system subsequently become one continuous column of urine (8).

If the obstruction is partial and the kidney continues to produce urine, the changes seen in the kidney are somewhat different. Atrophy of the tubules occur with longstanding obstruction, but the glomeruli remain intact unless the renal damage is very severe. The renal ability to concentrate urine remains low and the urine output from the affected kidney tends to be variable. Atrophy of the tubular cells also produces a loss of parenchymal mass. Ureteral peristalsis in partial obstruction is quite variable, ranging from complete absence of peristalsis to normal waves of peristaltic activity (3,9).

Grossly, the obstructed kidney has slight to massive enlargement in size. Simple dilatation of the pelvis and calyces are the earliest features of obstruction. Progressive blunting of the apices of the pyramids occur and eventually the apices become cupped. In advanced cases, the kidney atrophies down into a cystic, thin-walled structure with marked atrophy of the parenchyma, thinning of the cortex and obliteration of the pyramids (2).

Once the actual obstruction is removed, the collecting system proximal to it tends to revert towards normal. If the obstruction has been present for a short period of time, the ureter, collecting system and kidney often return to their normal, pre-obstructive state. If the obstruction is not relieved within a certain period of time, some element of ureteropelvic ectasia may remain and the parenchymal mass may remain diminished. The effects on the kidney depend primarily on the amount of tubular atrophy that has occurred. Unfortunately, atrophic parenchyma does not regenerate, so that even after the relief of obstruction the kidney may permanently remain nonfunctional (3). Studies have shown that irreversible, serious damage occurs after three months of incomplete obstruction and after three weeks of complete obstruction (10).

Obstruction at the bladder outlet is also a commonly recognized phenomenon. If severe urethral obstruction ensues and the mean pressure of the urine in the bladder is elevated, the peristaltic action of the ureters may not be sufficiently strong to propulse the urine into the bladder. When this happens, a continuous column of urine appears in the ureters and the pressure within begins to rise. Subsequently, the ureters and their corresponding collecting systems begin to distend. Once again, peristalsis becomes ineffective and may disappear entirely. This ureteral and collecting system distention is symmetrically bilateral since both ureters are exposed to the same bladder pressure.

Similar to ureteral obstruction, bladder-outlet obstruction may also produce hydronephrotic atrophy of the renal parenchyma and consequent irreversible damage (1).

ETIOLOGIES OF URINARY TRACT OBSTRUCTION IN THE PEDIATRIC POPULATION

In the pediatric population, the most common causes of urinary tract obstruction include ureteropelvic junction obstruction, ureterovesical junction obstruction, ureterocele, urethral valves and calculi (1). Ureteral obstruction in children may also occur by extrinsic pressure on the urinary system. These causes of extrinsic pressure include imperforate anus, intersex anomalies, Hirschsprung's disease, and tumor (2).

Ureteropelvic junction obstruction is the most common congenital obstruction of the urinary tract. It is found most often in male infants. It is most commonly seen on the left, but in up to 20% of cases, it can be bilateral. Possible etiologies include the abnormal organization of the smooth muscle fibers at the level of the ureteropelvic junction, an excess of collagen deposition between the smooth muscle fibers, compression by extrinsic intrauterine congenital bands, and aberrant renal blood vessels (3,4). Nowadays, most neonates with ureteropelvic junction obstruction present with a prenatal ultrasonographic diagnosis, an abdominal mass, or possibly a urinary tract infection. The presenting feature in older children is as an asymptomatic mass, a urinary tract infection, or an incidental finding on an abdominal image (3).

Obstruction of the distal ureter may be due to congenital or acquired ureterovesical junction obstruction. Congenital causes include ectopic insertion of the ureter, primary obstructive megaureter, simple ureterocele, and ectopic ureterocele.

Acquired etiologies include distal ureteral stricture following ureteral reimplantation, calculi, neurogenic bladder, edema and inflammation. Children with neurogenic bladders may develop dilatation of the urinary tract due to poor emptying, infection with vesicoureteral reflux, or obstruction from high sphincter pressures (3).

Ectopic insertion of the ureter is defined as the removal of the ureteral orifice some distance from its normal position on the trigone. The ectopic insertions can occur anywhere from the posterior urethra to the bladder neck or even to extravesical locations. Orifices at the bladder neck or in the posterior urethra may exhibit reflux of urine during voiding; however, they are usually obstructed because they empty into a predominantly closed space and are encircled by sphincteric muscle. In addition, ectopic ureters that insert outside of the urinary tract are almost always obstructed. More than two-thirds of all extravesical ectopic ureter insertions are associated with complete duplications of the collecting systems. In the male, the ectopic insertion of the ureter into the vas deferens and seminal vesicles is explained embryologically by the fact that these organs are derived from the mesonephric duct, from which the ureter is also derived. In 25% of all adult females remnants of the mesonephric duct can be found in the walls of the uterus, vagina and broad ligaments and thus explain the ectopic insertion of the ureter into these organs (2).

Primary megaureters can be both obstructed or nonobstructed. Obstructive megaureters are rarer and usually seen in infants and young children. The obstruction also more frequently involves the left ureter, but can be bilateral in up to 20% of cases. The obstruction is caused by a narrowed, aperistaltic ureteral segment ranging from 0.5 to 4 cm in length. The etiology is most likely due to the congenital absence of the spiral musculature with secondary local hypertrophy of the muscle. Associated fibrosis of the ureteral segment further limits the peristalsis and expansion (5).

Two types of ureteroceles can be identified in children. Simple ureteroceles are rarely diagnosed in children because they seldom produce signs of illness (3). Ectopic ureteroceles commonly present in children and represent the cystic dilatation of the ectopic ureters seen under the bladder mucosa. Ectopic ureteroceles are almost always associated with the upper moiety of a duplicated kidney whose ureter ends distal to the opening of the lower pole ureter. Ectopic ureteroceles are most often obstructed by their pinpoint orifices (3).

The most common cause of obstruction of the urethra in infants is posterior urethral valves. This is exclusively an abnormality of male infants. Fifty percent are discovered during the first three months of life (4). Three types of urethral valves have been described. All three types have the underlying defect of abnormal migration and insertion of the urethrovaginal folds which result in a sail-like valve that leads to obstruction of the posterior urethra. This obstruction causes severe dilatation of the posterior urethra and bladder hypertrophy and trabeculation with associated vesicoureteral reflux and subsequent hydronephrosis. The first type, Type I, consists of obstruction below the verumontanum, and is the most common. Type III is less common and is associated with a transverse diaphragm at the posterior urethra. The Type II valve is rare and is of questionable significance. Anterior urethral valves in males also exist, but are much less common (6).

Urinary stones are relatively uncommon in children. Four etiologic categories are usually identified in children: metabolic disorders, developmental anomalies with urinary stasis (with or without concomitant infection), immobilization, and idiopathic. In children with urolithiasis in whom infected urine is not found and who are not immobilized, complete diagnostic workup for metabolic abnormalities should be sought. These

abnormalities include renal tubular acidosis, hyperparathyroidism, cystinuria, or hyperoxaluria. Also, the child may have underlying pathology that produces excessive uric acid, such as Lesch-Nyhan syndrome, leukemia, or tumor lysis syndrome. If a child with urolithiasis is diagnosed with a urinary tract infection, some anatomic abnormality of the urinary tract should be sought. Immobilization is often deemed to be necessary after skeletal fracture in children. Unfortunately, it is accompanied by bone demineralization and consequent stone formation. Twenty-five to 45 percent of urinary stones in children are diagnosed as idiopathic. The stones are usually of calcium oxalate, although the urine does not show evidence of possessing excretions of any crystalloid. The condition is thought to be genetic in origin and to result from a primary renal defect in the handling of calcium. Interestingly, in the past, the diagnosis of urolithiasis under the age of one was unknown. However, in the neonate, stones are now being diagnosed in premature infants after long-term furosemide therapy for the respiratory distress syndrome (7).

OTHER CAUSES OF HYDRONEPHROSIS

Although urinary tract obstruction is usually manifested by hydronephrosis, one must remember that several other etiologies may also present as hydronephrosis in children. Vesicoureteral reflux, for example, is a common cause of an enlarged pelvicalyceal system in children. In fact, upon initial screening, it may be indistinguishable from obstructive hydronephrosis (1). Vesicoureteral reflux is defined as the "regurgitation of bladder urine into the upper urinary tract" (2). As described earlier, the oblique entry of the ureter as it enters the bladder, the length of the submucosal segment of the intramural ureter, and the support of the detrusor muscle are the anatomic features that define the normal valve mechanism of the ureterovesical junction. With

vesicoureteral reflux, the underlying defect is a congenital abnormal ureteral submucosal tunnel at the ureterovesical junction (3). The effects of vesicoureteral reflux are many and include renal dysplasia, recurrent infections of the urinary tract, renal scarring, decreased renal growth, hydrostatic damage, chronic renal failure, and hypertension (4). Chronic vesicoureteral reflux with infection causes reflux nephropathy, consisting of damage to the papillae, calyceal blunting and cortical scarring (3).

Another cause of nonobstructive dilation of the pelvicalyceal system is congenital nonobstructive megaureter, in which the ureter is often dilated from kidney to bladder. The dilatation can involve the entire ureter or it may be segmental, particularly distally (5). Obstruction cannot be identified and surgical correction is usually not necessary. The cause of nonobstructive megaureter is idiopathic, however, the failure of the ureteral walls to coapt does not allow for effective peristalsis. This defect leads to stasis, intermittent infection and varying degrees of concomitant hydroureteronephrosis (6). However, many cases diagnosed in early childhood remain stable or even improve with observation alone (5).

Congenital megacalyces is a condition where there is unilateral polygonal enlargement of the calyces, with no associated dilatation of the renal pelvis or ureter. In addition, there is no history of obstruction, pain or infection. However, investigators feel that a great majority of kidneys with megacalyces have once been subjected to either reflux or obstruction at some point in time, possibly even during fetal life (7).

Prune belly syndrome, also known as Eagle Barrett syndrome, is considered a fourth cause of nonobstructive hydronephrosis in male children. It is a congenital disorder manifested by the absence of the abdominal wall musculature, cryptorchidism, and urinary tract dilatation, particularly of the lower ureters, bladder and prostatic urethra.

Clinically, the syndrome is recognized by the wrinkled, prune-like appearance of the abdomen and a small, empty scrotum. In girls, absence of the abdominal wall musculature as well as urinary tract anomalies may be seen and are therefore called "pseudoprunes". The posterior urethra is abnormally dilated, the bladder is distended and large, and the ureters are markedly tortuous and dilated, and can sometimes even be palpated (8). The etiology of the prune belly syndrome is most likely the failure of the lateral somite mesoderm to migrate and develop into the abdominal wall musculature and that of the urinary tract, possibly the result of transient early fetal urethral obstruction that spontaneously remits (9).

Other causes of nonobstructive hydronephrosis in children include infection, myelodysplastic kidneys, the megacystis-microcolon-intestinal hyperperistalsis syndrome, residual dilation from previous obstruction, and polyuria associated with acute diuresis and diabetes insipidus (10). Thus, it is important to remember that not all wide ureters and dilated collecting systems are either obstructed or refluxing.

PART III

HISTORY OF DIAGNOSTIC ULTRASOUND

Six major periods can be identified in the history of diagnostic ultrasound. The first period began in 1880 with Pierre and Jacques Curie, brothers who experimented with the development of high frequency sounds and developed the concept of the "piezoelectric effect." This phenomenon is based on the observation that certain asymmetric polycrystalline metals and natural salts will produce an electrical current when stressed mechanically. Subsequently, in 1881, the Curie brothers discovered that by stimulating the piezoelectric crystal with an oscillating current, pressure waves above human hearing range occurred in the crystal, a phenomenon they labeled the "reverse piezoelectric effect" (1). The use of the piezoelectric and the reverse piezoelectric effects is the basis for the transmission and reflection of sound energy in the ultrasound used today for medical diagnosis (2).

The second period took root during 1912, with the sinking of the U.S.S. Titanic. Scientists began to search for methods to detect underwater obstacles. In 1917, Legevin, a French scientist, developed a technique that allowed ultrasonographic pulses to be passed through water and to be reflected from underwater objects. The purpose of this technique was for submarine detection and subsequently, this became what is known today as SONAR (SOund NAvigation and Ranging), a principle which was in widespread use during World War II. Modifications of Legevin's technique are used today as depth finders for mapping the ocean floor and for locating schools of fish (3).

The third period, which began in 1935 and extended to 1952, is loaded with controversy regarding the origin of the pulse-echo flaw detection technique, the principle

upon which diagnostic ultrasound is based (3). In 1935, Sokolov described the use of sound to detect flaws in solid objects . He measured the transit time of the sound (through the back and front of the material) and any delay in the transit time was an indication of a flaw in the object (4). Although the implication of "pulse-echo" technique was there, Sokolov neither specifically related to "echoes" from the flaws in the material nor stated that this technique was actually "pulse-echo." In 1939, Sokolov patented a technique for the detection of flaws in metals based upon the use of continuous waves of ultrasound in association with a through transmission technique (5). However, it was not until 1940 that the "pulse-echo" technique was truly discovered by Firestone. At that time, he patented a flaw detection device, which he called "the Reflectoscope", in which ultrasound waves were passed through the object which was being examined. When a flaw was detected by the device, sound was reflected and an electronic signal appeared on a cathode ray tube (6). Unfortunately, because Firestone's work was considered classified information during the era of World War II, it could not be published until 1946, when security restrictions were ended (3).

The first application of diagnostic ultrasound techniques in medicine was a through transmission technique, first described by Dussik of Vienna in 1937. He transmitted ultrasound from a transducer through a patient's skull to a receiving transducer. The varying intensities of the transmitted ultrasound which were detected by the receiving transducer controlled the intensity of a lightbulb and a photographic image would be produced showing areas of higher amounts of transmitted ultrasound and of decreased transmission as white and black, respectively. Dussik hypothesized that the ultrasound would pass through the skull and brain and that there would be a loss in the transmitted ultrasound once it passed through the cerebral ventricles (3). Using a similar technique, Ballentine et al. came to the same conclusion (7). However, in 1952, Guttner et al. concluded that the differences in the transmitted signal should not be attributed to

the attenuation by the cerebral ventricles but rather to the cranial vault (8). Thus, it seemed like the short-lived age of ultrasound had come to its end.

Fortunately, the fourth period had begun three years earlier, in 1949, when Struthers and Ludwig started implanting foreign bodies within the muscles of dogs and attempted to detect them ultrasonographically. They obtained a variety of echoes and concluded that this procedure was certainly feasible (9). For the next several years, the majority of the ongoing research centered in Minnesota. Wild demonstrated a significant difference between the echoes of normal canine small bowel thickness and those of pathological bowel thickness (10). He continued his research and discovered echoes from a tumor in an excised brain and subsequently, confirmed the same phenomenon in the brain of a living subject across an intact scalp through a craniotomy (11). Wild continued his work on investigating intact human tissue by studying tumors within the human breast. He collaborated with Reid, an engineer, and through one-dimensional (A-mode) methods as well as by measuring the area under the graphic representation of the echoes, was able to distinguish between benign and malignant breast tissue. Of 21 patients examined, they correctly diagnosed 12 out of the 14 malignant breast lesions (12). Wild and Reid subsequently went on to design the first equipment to examine tissue in two dimensions, the B-mode scanner in 1951 (13).

At about the same time that Wild and Reid were performing their investigations, Howry and Bliss of Colorado were designing the first pulse-echo system made for clinical use. The naked subject was submerged and weighed down in a laundry tub while the transducer rotated through the water and one-dimensional images of the lower abdomen were obtained. However, these images were unfortunately crude and incomplete. In 1951, they discovered that moving the transducer in two different planes resulted in clearer, impressive and anatomically correct images. This heralded the

beginning of the compound scanner (14). In 1954, they began to image the upper abdomen, such as the liver, spleen and kidneys. With increasing experience, they developed the "pan-scanner", which allowed the patient the freedom to sit alongside, rather than inside, the tank which contained the transducer. Ultimately, the compound contact scanner was developed which could scan the subject directly albeit with the use of lubricating gel to replace the cumbersome water-path (15).

In 1955, diagnostic ultrasound was forced into a period of hibernation due to a report published by the Atomic Energy Commission which reported that "ultrasonics" were "unsuitable" and "foolish" for detecting intracranial lesions. This statement brought the fourth period of diagnostic ultrasound to a close (3).

The fifth era of ultrasound was concentrated mostly in Europe and Japan, and due to the Atomic Energy Commission, very little American investigation was pursued. Echocardiography was born in 1954 in Sweden due to the work of Edler and Hertz (3). By using basic unidimensional information and electronically modifying this information, they detected pericardial effusion, mitral valve disease and atrial tumors. This constituted the first M-mode recordings. Very shortly after, Leskell, also from Sweden, described the A-mode technique of echoencephalography, while attempting to demonstrate the presence or absence of a shift of the midline structures of the brain (3). In 1956, Satomura of Okasa University in Japan was the first to describe the ultrasonographic Doppler effect (16).

In the 1960s, the clinical application of sonography was seen mainly in two medical specialties, namely, ophthalmology and neurology / neurosurgery. The enthusiasm of the ophthalmologists resulted from the double benefits of ultrasonic energy which helped them to visualize deep ocular structures and gave them an accurate axial

measurement of imaged interfaces. The neurologists discovered that sonography could image the internal anatomy of the brain which was a major advance since simple x-ray transmission images of the brain were obscured by the overlying skull (16). The predominance of sonography in these two specialties is apparent by the fact that up to the end of the 1960s, 1337 publications concerning sonography in ophthalmology and neurology were published which exceeded the 1014 publications in all other ultrasonic diagnostic fields, including echocardiography, obstetrics, and abdominal imaging (17).

As mentioned previously, the static two-dimensional B-mode scanner was developed in 1951. However, a single image could take several minutes to form and even worse, if any of the tissues under examination were to have moved, a distorted image would have resulted. Thus, in the mid-1970s, the beginning of the sixth period, a series of motor-driven high-speed methods and electronically controlled alternatives were described. With these methods, image formation lasted only 0.1 seconds. These images taken in series gave the impression of "real-time" motion and thus, were called "real-time" methods of ultrasonography. These methods were seen commercially between 1975 and 1980 (18).

In the latter half of the 1970s, "real-time" two-dimensional B-mode imaging instruments stabilized and multigated pulsed Doppler systems were developed using phase demodulation. Time domain frequency analysis as well as spectral waveform analysis and standard video display formats were constructed. The 1980s showed improved "real-time" B-mode imaging with high-density linear arrays, phased arrays and annular arrays. However, the most exciting development in the 1980s was the commercialization of color flow imaging, which simplified the task of locating blood vessels (18).

The application of ultrasound techniques to the field of urology is a relatively new achievement, since the early days of uroradiology were dominated by the urologists (19). Even before the intravenous urography, retrograde pyelography was the primary radiologic diagnostic method for evaluating the upper tracts and this was in the realm of urology. Intravenous urography was discovered by urologists, and despite its availability, retrograde pyelography maintained its position of dominance until the 1960s when selective angiography, drip infusion pyelography, high-dose intravenous urography, and nephrotomography placed radiologists in charge of uroradiology. Radioisotope renography developed in 1956, was the beginning of nuclear medicine for the urinary tract (20). Ultimately, in the late 1970s and early 1980s sonographic techniques and computed tomography became readily available in the field of uroradiology, which reflected the enormous potential that noninvasive imaging and examination of blood flow offers in this area (19).

PHYSICS OF DIAGNOSTIC ULTRASOUND

Ultrasonographic imaging is performed by using the pulse-echo technique (Figure 1). The transducer used in ultrasonography converts electrical energy into a short pulse of high-frequency sound energy that is transmitted into tissues. The transducer then becomes the receiver of this energy, detecting echoes of sound reflected from the tissues. The depth of the echoes is determined by the time of the round-trip flight for the transmitted pulse and the returning echo, with the assumption that the average speed of sound in tissue is 1540 m/sec. The ultrasonographic image is produced by interrogating tissue in the field of view with multiple close ultrasound pulses (1).

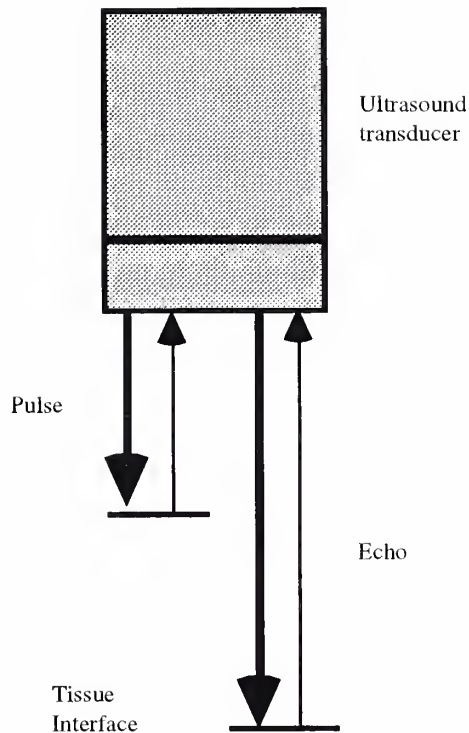


FIGURE 1. The Ultrasound Pulse-Echo Technique. The sonographic transducer transmits a short pulse of ultrasound energy into the tissue. The transmitted pulse encounters tissue interfaces that reflect a portion of the sonographic beam back to the transducer (Brant, W.E. *Diagnostic Imaging Methods*. In Brant, W.E. and Helms, C.A. (Eds.) *Fundamentals in Diagnostic Radiology*, 1994, p.13).

Sound consists of longitudinal vibrations that propagate through a medium such as soft tissue by a series of oscillating compressions and rarefactions of the molecules in the medium. Ultrasound is the longitudinal vibrations which occur at frequencies greater than 20,000 Hertz, which is above normal human hearing range (2). The number of compressions produced each second is known as the frequency (f); the distance between the successive compressions is known as the wavelength (λ), and the acoustic velocity (c) is the velocity of the vibrations as they propagate through a medium. These three variables are related mathematically by the equation: $C=f\lambda$ (2).

Echoes arise when a sequence of ultrasound encounters an interface between structures that differ in their acoustic impedance. Acoustic impedance (Z) is a mechanical property that is defined as the product of the density (ρ) of tissue and the speed (c) at which sound propagates through it. Mathematically, this is expressed as $Z = \rho c$. The speed of sound is influenced by the stiffness of the tissue through which it passes. Thus, in reality what ultrasound imaging does is to map the changes in the mechanical property of tissues. Furthermore, the variation in the structure of tissues at the cellular level results in changes in its acoustic properties, including impedance. Hence, ultrasound turns out to be a valuable method for imaging soft tissue structures (3).

When sound encounters a second medium of a different impedance, part of the wave is reflected back to the source of the sound and the rest passes through the second medium. The reflection coefficient is the amount of sound that is reflected from the reflecting tissue interface of the source. Mathematically, it is defined as:

$$R_c = \frac{(Z_2 - Z_1)^2}{(Z_2 + Z_1)^2} \quad \text{where } Z_1 \text{ is the impedance of tissue one and } Z_2 \text{ is the impedance of}$$

tissue two. The calculation of the reflection coefficient assumes that the ultrasound beam strikes the interface between the media at a right angle. If it does not, and this is usually the case, the amount of ultrasound reflected to the transducer is reduced. If the two media have equal impedance's, there will be no reflection because $Z_2 - Z_1 = 0$. The larger the difference in impedance, the larger the reflection coefficient and the stronger the echo will be (3).

The most accurate way to measure the time period between interfaces is by displaying the echoes as deflections on a cathode ray tube. A spot is made to traverse the screen of the cathode ray tube quickly from left to right and the electrical signal from the

transducer causes a vertical deflection. The acoustic pulse that is generated travels into the tissue until it meets an interface where the impedance changes from where the reflection gives rise to an echo, which travels back to the transducer. When the echo then reaches the transducer, a signal is produced that causes a second deflection of the spot on the cathode ray tube screen. This one-dimensional trace with echo amplitude on the vertical axis and depth on the horizontal axis is known as an A-mode scan (2) (Figure 2).

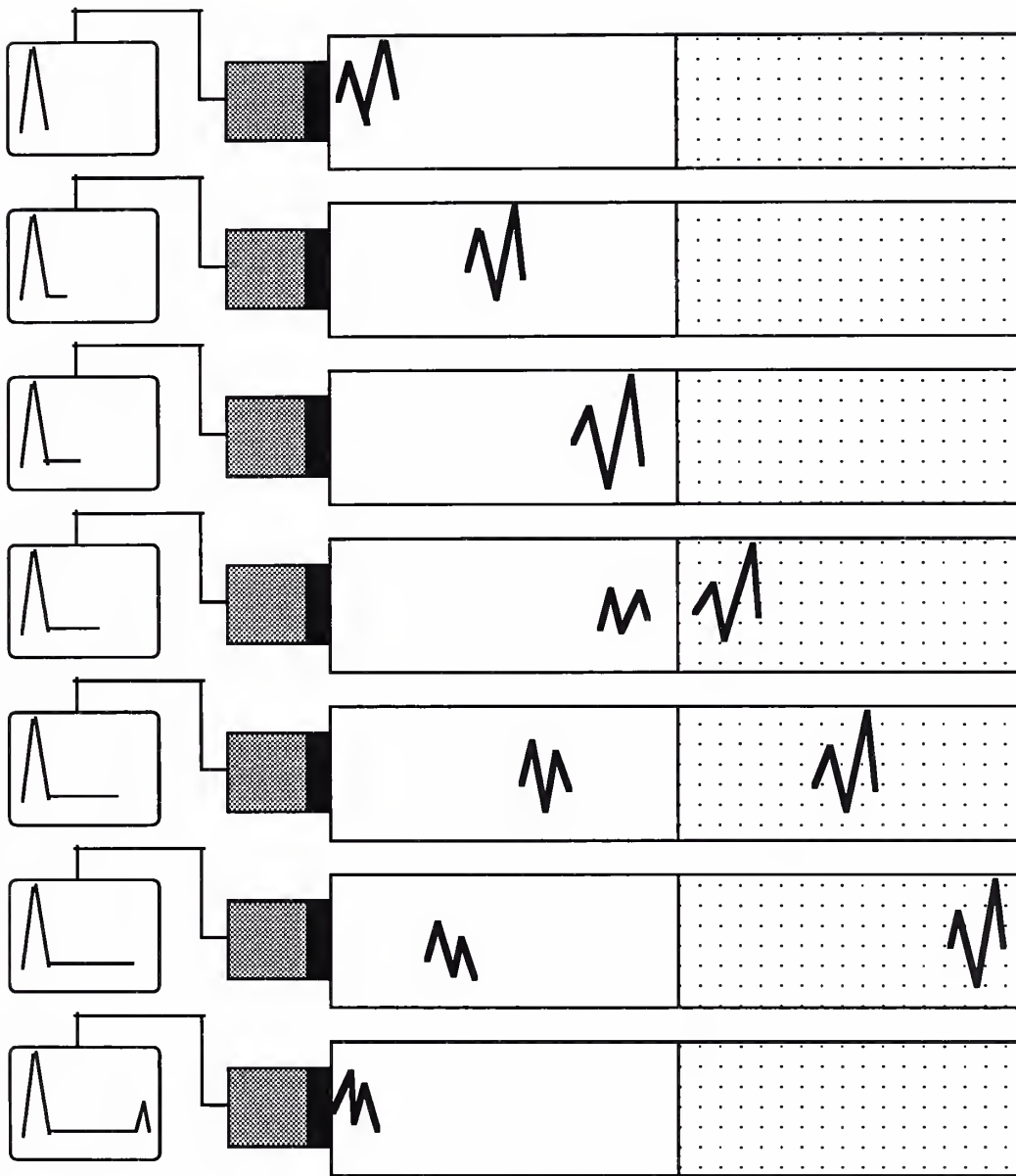


FIGURE 2. The Ultrasound A-Scan. The pulse-echo principle is used to produce the ultrasound A-scan. A pulse is sent from the transducer at the same time as a dot is set in motion from left to right on the A-scan screen. When the echo reaches the transducer, the signal causes a vertical deflection of the trace. The distance between the deflections on the A-scan corresponds to the depth of the interface from the transducer (Burns, P.N. *Ultrasound Imaging and Doppler: Principles and Instrumentation*, In Resnick, M.I. and Rifkin, M.D. (Eds.) *Ultrasonography of the Urinary Tract*, 1991, p.2).

The echoes can also be imaged as dots in a straight line, with their brightness proportional to the echo amplitude. If the transducer is mounted on a position sensing arm, the acoustic beam line of view can be made to correspond to the orientation of the A-scan line on the display screen. The movement of the arm across the skin surface will then produce a series of dots which correspond to the cross-section of the interface within tissue. The image formed is called a B-mode image. This two-dimensional image forms the basis for the modern ultrasound machines (2).

The major components of an ultrasound imaging system include a clock which initiates the sequence that results in a single image seen on the screen. A pulse is then created by the pulse generator (piezoelectric crystal) and sent by the transducer. As the echoes are subsequently received by the transducer, they are amplified and demodulated to determine their strength. Because the sound is pulsed, the two functions of transmitting and receiving sound waves are separated in time so no interference is seen between the two entities. The group of echoes is then presented to the scan converter, which is a type of memory that stores the echoes as well as their orientation and time of arrival. The data are then read from the memory in a television raster format and changed to a video signal on the imaging monitor. As soon as all of the echoes are received, the clock initiates another sequence (2). Thus, as the transducer is moved over the patient, images are formed (Figure 3).

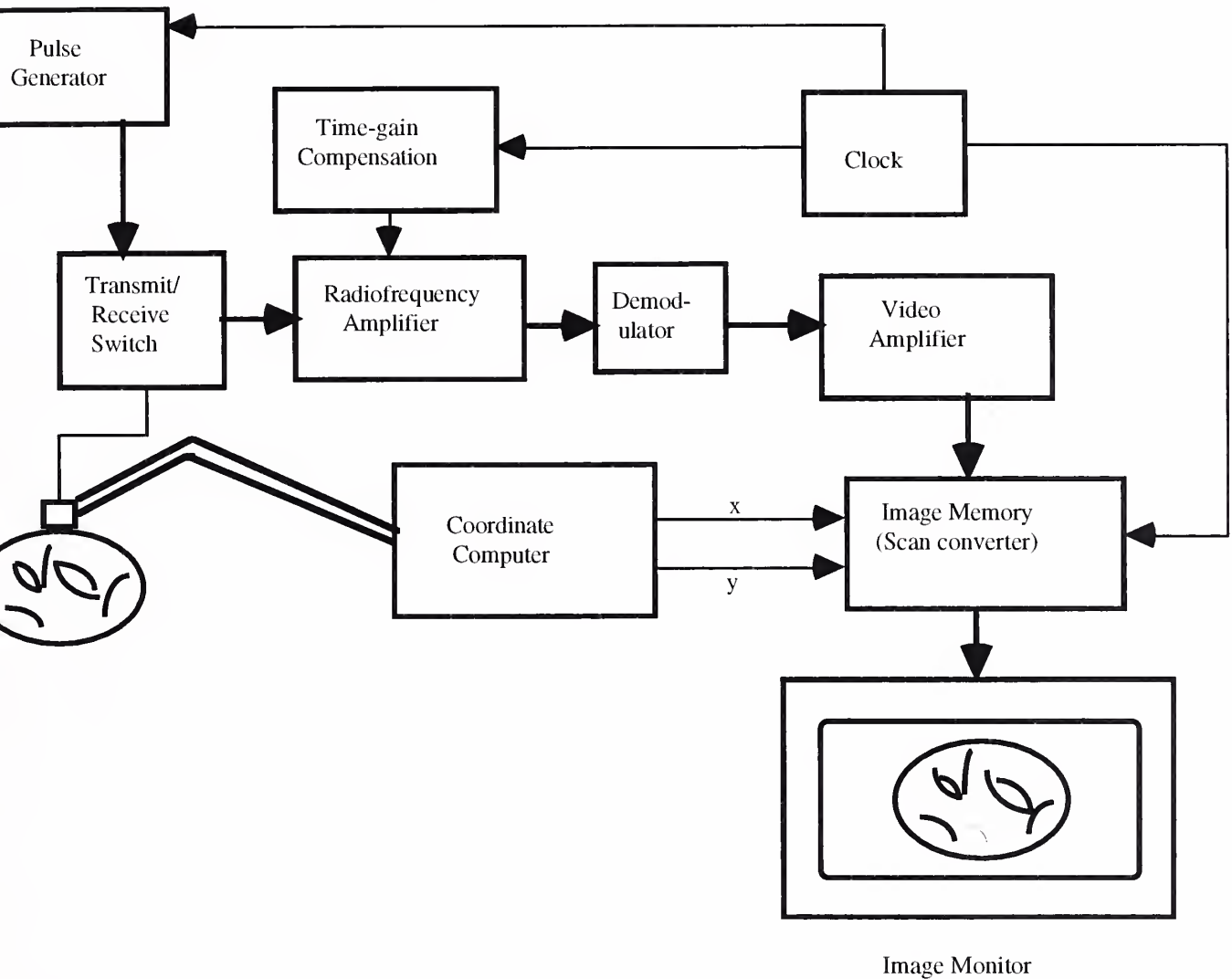
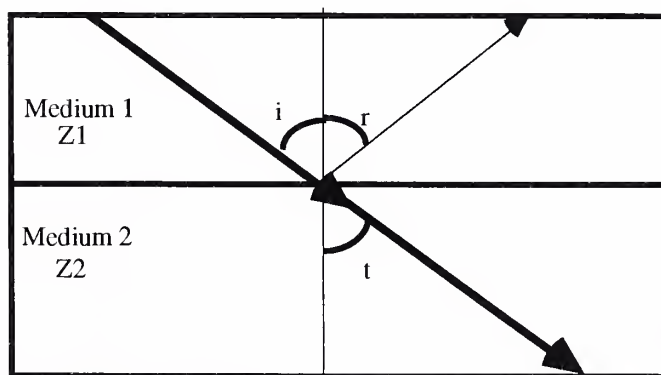


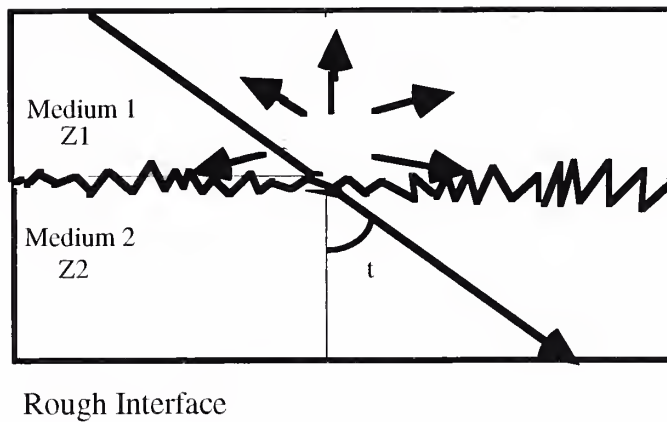
FIGURE 3. The major components of an ultrasound imaging system. A pulse is first issued by the pulse generator and emitted by the transducer. The direction of orientation of the transducer is assessed by the coordinate computer and sent to the scan converter. As the echoes are received from the tissue, they are amplified and demodulated to measure their strength. Individual echoes are represented as lines in the appropriate direction and their brightness is modulated on the image monitor. As the transducer moves, an image is produced on the monitor (Burns, P.N. *Ultrasound Imaging and Doppler: Principles and Instrumentation*, In Resnick, M.I. and Rifkin, M.D. (Eds.) *Ultrasonography of the Urinary Tract*, 1991, p.5).

If the transmitted pulse is reflected from a smooth surface the ultrasound echoes are considered to be specular and echoes will only be seen if the beam is perpendicular to the surface. These surfaces are seen at tissue boundaries as well as the walls of major vessels. If the pulse is reflected from an irregular surface, the echoes are produced in many directions. This scattered waves also contribute to the image and are the basis for the visualization of tissue margins. Also, small differences in the impedance of the parenchyma of the tissue also give rise to low-level scattering. The intensity and structure of these backscattered echoes form the basis for gray-scale ultrasonography (2) (Figure 4).

FIGURE 4. The difference between specular and rough interface reflection. Ultrasound pulses encounter interfaces between soft tissues of differing acoustic impedance. In specular reflection, a small portion of the ultrasound beam is reflected but most passes across the interface undeviated. The angle of incidence (i), the angle of reflection (r) and the angle of transmission (t) are all equal. When the interface is rough, specular reflections from the irregularly oriented edges gives rise to echoes over a range of angles. As sound propagates through the parenchyma, small quantities of ultrasound are scattered in all directions, including back toward the transducer. This forms the gray-scale appearance of the organ (Burns, P.N. *Ultrasound Imaging and Doppler: Principles and Instrumentation*, In Resnick, M.I. and Rifkin, M.D. (Eds.) *Ultrasonography of the Urinary Tract*, 1991, p.6,7).



Specular Reflection



Attenuation of the ultrasound pulse in tissue is the result of the absorption of the pulse by tissue, converting the energy into an immeasurably small quantity of heat. Attenuation is dependent on frequency and it reduces the intensity of the pulse logarithmically as it passes through the tissue. The effect of attenuation is a reduction in the intensity of returning echoes from deeper tissues. However, the receiver compensates for this loss by increasing its gain logarithmically as the echoes arrive from the deeper structures. The gain is increased throughout the period in which the echoes from the deeper structures arise. Thus, echoes of equal strength from differing depths are seen with the same intensity on the screen. This is called time gain compensation (2).

Axial resolution is defined as the minimum separation between two targets in tissue parallel to the beam that allows the distinction between two separate structures. The main factor that determines axial resolution is the spatial ultrasound pulse length. The pulse length is defined as the product of the number of cycles per pulse and the wavelength of the sound. The shorter the pulse length the better the resolution. Increasing the frequency or decreasing the wavelength enhances the axial resolution. However, as the frequency increases, the penetration depth decreases and thus, one must compromise resolution for adequate tissue penetration. Lateral resolution is defined as the minimum separation of two targets in tissue, located along a direction perpendicular to the

ultrasound pulse, that results in the imaging of two separate structures. The main determinant of lateral resolution is the width of the ultrasound beam. The precision of a measurement obtained in the lateral direction varies according to depth, the size of the transducer and the degree of focusing achieved. In general, higher frequency transducers produce narrower beams, so that lateral resolution improves with increasing frequency and decreasing wavelength. However, this also results in a decreased depth of sound wave penetration of tissues as was seen with axial resolution (4).

The transducer attached to an arm has been replaced in modern ultrasound equipment by a transducer using a mechanical rotator or translator. The beam is moved with great speed so that an entire image can be created in fractions of a second and independent images may be acquired quite quickly. The display of these images in rapid succession allows the production of real-time images of moving organs which allows for the evaluation of ureteral peristalsis, for example. The M-mode, for movement, is the recording of movement of a single space dimension in time. It is most commonly utilized in echocardiograms (2).

DOPPLER ULTRASOUND

In 1842, Christian Doppler theorized that the frequency of either sound or light when emitted or reflected from an object in motion will vary with the velocity of the object (1). The acoustical Doppler effect occurs whenever there is relative motion between the source and the receiver of the sound. Doppler physics as it relates to diagnostic ultrasonography involves the behavior of high frequency sound waves as they are reflected from a moving target. In clinical imaging the moving objects of interest are the red blood cells in flowing blood (2). Hence, Doppler methods are special among those

clinical techniques in diagnostic ultrasound because they have the potential to offer information related to the function of an organ rather than its morphology.

When high frequency sound is reflected from a moving target, the frequency of the reflected wave received differs from that of the transmitted one. This difference in frequency is known as the Doppler shift, and depends upon whether the motion is toward or away from the receiver as well as the speed at which the target is moving. The reflected frequency which is received by the transducer from a moving object can be calculated mathematically from the following equation: $f_{\text{eff}} = f_o (c \pm V_r) / c$, where f_{eff} is the received frequency, c is the acoustic velocity in the tissue, f_o is the transmitted frequency and V_r is the target velocity. The sign is positive if the reflector is moving toward the transducer and negative if the reflector is moving away from the transducer. When speaking about ultrasound, the source and receiver are the same, and thus, the Doppler shifts are equal and simply add to each other. Mathematically, this is expressed as: $f_D = 2fv \cos \vartheta / c$, where f_D is the Doppler shift, f is the transmitted frequency, v is the target velocity and ϑ is the angle between the direction of movement of the reflector and the ultrasonic beam. In the extreme case where the motion is aligned precisely with the beam, the angle is equal to 0° or 180° and thus, the Doppler shift is at its maximum. Conversely, if the motion is perpendicular to the beam, the angle is equal to 90° and no Doppler shift is produced (3).

It is a fortunate coincidence that for the range of ultrasound frequencies used clinically, the range of tissue velocities encountered physiologically and the velocity of sound in blood, the range of Doppler shift frequencies in most medical applications happen to lie in the human audible range. Thus, it is quite convenient that the Doppler flowmeter converts the shift frequency into an audible signal that can be monitored (4).

The simplest instrument used in Doppler imaging is the continuous wave Doppler shift detector, where sound is continuously emitted from one transducer and a continuous stream of echoes arrives at the receiving transducer. The two transducers are housed together with their beams overlapping. Because of the continuous wave form, Doppler signals from all depths of the beam patterns will be detected. Thus, the presence of several vessels within the beam patterns allows for the superimposition of several Doppler signals. Thus, continuous wave form Doppler is only of clinical use in certain areas of the body, such as superficial structures with only one moving structure within the sound beam such as in the examination of the carotid artery and superficial vessels of the limbs. In addition, continuous wave Doppler is capable of very high sensitivity to weak signals and so is clinically useful in the examination of smaller vessels such as the ophthalmic and supraorbital arteries and those supplying the female breast. These limitations unfortunately preclude the use of continuous wave Doppler for blood flow measurements in the abdomen and retroperitoneum (4).

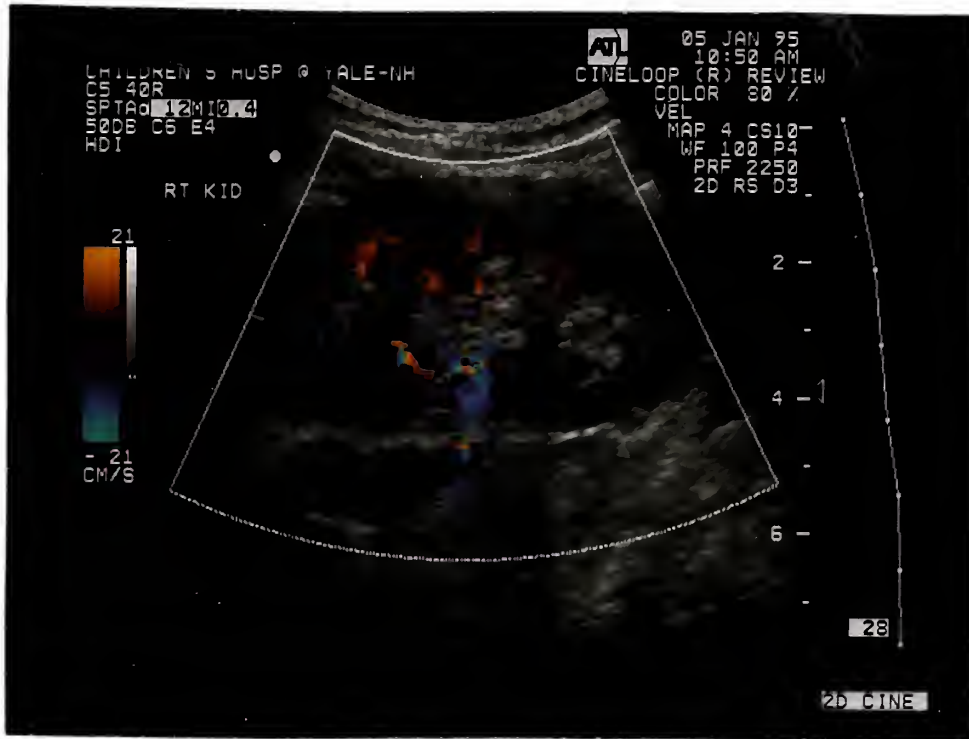
Pulsed Doppler systems combine the detection of velocity seen in the continuous Doppler system with the range discrimination of a pulse-echo system. Bursts of ultrasound are transmitted at regular intervals and a continuous stream of echoes are reflected back to the transducer. The same transducer is used for transmitting and receiving. The range of the tissue at which the Doppler signals are detected is controlled by changing the length of time that the system waits after sending a pulse before opening the gate that allows the returning signals to be received. Thus, pulsed Doppler can be used to determine blood flow in a vessel at a given depth when there is more than one vessel within the beam. However, there is an upper limit to the amount of Doppler shift that can be detected by the pulsed Doppler instruments, which is not seen with the continuous Doppler systems. When this limit is exceeded, erroneous Doppler shift information is generated, called "aliased" signals (5).

The combination of real-time imaging and Doppler techniques is known as duplex scanning. Usually, modern duplex scanners involve a combination of real-time imaging and pulsed Doppler to identify the volume in tissue from which Doppler frequencies are received. A duplex scanner does not perform imaging and Doppler measurements simultaneously. Usually, the real-time image of the area which contains the vessels or structures of interest is detected and then the system is switched to Doppler mode and the interrogation with the Doppler system is initiated. With mechanically steered systems, it is not readily feasible to switch from the imaging and Doppler modes very quickly and so the image is usually "frozen" on the screen while the Doppler signals are collected (4). However, with electronic scanning using arrays rapid switching between the imaging and Doppler functions is possible, allowing apparent simultaneous acquisition between Doppler flow information and real-time images (5). A powerful advantage of the duplex system is that it allows for the estimation of the velocity of flow from the Doppler shift frequency (4).

Doppler flow information can also be presented in a manner similar to real-time sonography of anatomic structures. This is done by using a pulse-echo technique similar to that used for gray-scale imaging. However, rather than displaying the reflected echoes with gray-scale hues, these echoes are projected in color. Thus, color flow Doppler imaging combines gray-scale and Doppler information in a single image. Those tissues that are stationary with echoes having no Doppler shift are seen in shades of gray, while blood flow and tissue that is in motion which produce detectable Doppler signals are displayed in color (Figure 5). The colors utilized are usually of two tones with the brightness, saturation or hue of the colors used to distinguish different velocity magnitudes both toward and away from the transducer. Blood which flows towards the direction of the transducer is usually displayed in shades of red, while blood flowing away from the transducer is seen in shades of blue. Colors of lighter shades imply a

higher flow velocity. Turbulent flow is usually represented by the color green and is determined by the variance in flow (5).

Figure 5. Color flow Doppler imaging. Clinical example of color-flow doppler showing opposite flow directions in the intrarenal vessels. The color map setting is indicated by the bar on the left side of the image. The segmental and interlobar arteries appear in red, and the corresponding veins in blue.



The fundamental tool for the analysis of Doppler wave forms is the spectrum or frequency analyzer. This equipment is capable of distinguishing the relative powers of the different frequency components in the signal at any given time. The most common method for implementing spectral analysis is the digital fast Fourier technique (FFT). Short periods are analyzed mathematically for their frequency components and are displayed as a sonogram, in which a single spectrum is displayed as a vertical line on whose axis lies frequency with brightness modulated at each point to represent amplitude. The subsequent spectra are depicted as vertical lines at a fixed distance apart, displaying an image that is scrolled from left to right with time. Thus, the three variables of time,

frequency and amplitude are shown in real time, which is called the time-velocity profile (4).

Doppler ultrasound can assess the pattern of flow both qualitatively and quantitatively. Qualitative methods include the assessment of the presence of flow, the direction of flow and the identification of characteristic flow in various parts of the circulation. Flow conditions at the site of measurement are indicated by the width of the spectrum with broadening of the spectrum indicative of turbulent flow. Blood flow can also be measured by more quantitative measurements. Turbulent flow can be distinguished from laminar flow by their respective Doppler signals. Flow conditions downstream, especially distal flow impedance, are seen by the relationship between the peak systolic and end diastolic flow speeds. Various indices for quantitatively presenting this information have been developed. These indices are a ratio of two Doppler shift frequencies and are independent of the Doppler angle and thus, pulsatility can be assessed in vessels that are too tortuous or too small to be imaged. The ratios are used to define an index of pulsatility to the waveform that can be used as indicators of distal impedance. The higher the distal impedance, the more pulsatile the waveform. The most common ratios used include:

$$\text{Pulsatility index} = (A-B) / \text{mean}$$

$$\text{Resistance index} = (A-B) / A$$

$$\text{S-D ratio} = A/B$$

where A is the maximal Doppler shift frequency over the cardiac cycle, B is the minimal Doppler shift frequency, and the mean is the time average of the maximal Doppler shift frequency over the cardiac cycle (6). The pulsatility index is the ratio that is least susceptible to variation due to heart rate and is considered the strongest of the indices. However, it is the least convenient to measure since it requires the digitalization and area integration of the entire time-velocity waveform (4).

PART IV

PRENATAL SCREENING OF HYDRONEPHROSIS

Screening of the urinary tract by ultrasonography may begin long before the birth of a child. Altered growth of the fetus in addition to a wide variety of fetal abnormalities can presently be diagnosed by maternal ultrasonography. The dilated fetal urinary tract is a finding seen frequently on ultrasound and is associated with a wide range of prognoses. Mild dilatation of the tract usually remains stable after birth or resolves entirely. Greater degrees of dilatation are often associated with partial or complete urinary tract obstruction which may lead to neonatal renal failure (1).

Aspects of the fetal urinary tract can be identified as early as 15 weeks gestation. However, the definition of the renal architecture is oftentimes not possible until the 20th week when the obstetrician is able to assess the anteroposterior diameter of the fetal renal pelvis, the diameter of the kidney, and the degree of pelvicalyceal dilatation (2). These parameters have been correlated with gestational age. The fetal bladder is also readily seen early in the second trimester (3).

Dilatation of the fetal urinary tract frequently, but not necessarily, heralds obstruction (4). It is also quite possible for obstruction to be present in the absence of urinary tract dilatation. The ultrasonographic findings consistent with obstruction include fetal bladder enlargement, hydronephrosis and hydroureter with or without dysplastic renal degeneration (5). Obstructive uropathy is identified as unilateral or bilateral and is divided according to anatomical level. Obstruction of the superior urinary tract may be seen sonographically as a dilated renal pelvis only and may signify ureteropelvic junction obstruction or ureteral atresia. Mid-level obstruction is visualized as ureteral dilatation

with or without a dilated renal pelvis and ureterovesical junction obstruction, bladder atresia, or transient hydroureter may be the underlying etiology. Obstruction of the inferior urinary tract is seen as a dilated bladder and proximal urinary system and may signify posterior urethral valves, urethral atresia or persistent cloacal syndrome (1).

At least three non-obstructive anomalies of the urinary tract may present with prenatal sonographic features similar to those seen in obstruction. Differentiation between the etiologies is quite difficult, but is important because *in utero* intervention for non-obstructive disorders is not indicated. As previously mentioned, massive bilateral reflux causes hydroureter and hydronephrosis which can be identified with prenatal ultrasound. The bladder is usually normal in size, although hypertrophy may occur. The megacystis microcolon-intestinal hyperperistalsis syndrome (MMIH) may also be confused with urinary tract obstruction. It is seen sonographically by megacystis, hydroureter, and bilateral hydronephrosis. Finally, the prune-belly syndrome is a condition that is also characterized sonographically by megacystis, hydroureter and variable degrees of hydronephrosis, but with the addition of the absence of abdominal wall musculature (1).

Obstetrical diagnostic and management challenges start by attempting to differentiate true obstruction from non-obstructive causes of hydronephrosis. If, indeed, a true obstructive uropathy is suspected, the obstetrician must then try to determine the etiology and pathophysiology of the obstruction. Research has suggested that *in utero* relief of the obstruction during the most active period of nephrogenesis (20-30 weeks gestation) may inhibit further damage to the kidneys and allow renal development to proceed normally (6). The combination of sonographic and physiologic criteria, such as GFR estimation and the specific gravity of the urine, identifies those fetuses most likely to benefit from therapeutic intervention. Rigid criteria for selection of patients for intervention are necessary because significant risks of chorioamnionitis, abdominal wall

defects, and pre-term labor are highly associated with intervention therapy (1). Usually, most fetuses suspected of having a unilateral obstruction are referred for postpartum ultrasonographic scanning to determine whether or not the urinary tract dilatation has worsened or has been relieved.

DIAGNOSIS OF URINARY TRACT OBSTRUCTION IN THE PEDIATRIC POPULATION

As discussed above, many newborns with hydronephrosis are being identified prenatally with the use of antenatal ultrasound. Thus, in recent years radiologists and clinicians have been confronted with an increasing number of neonates with prenatally diagnosed urinary tract dilation in whom the underlying significance and pathology are difficult to interpret (1). Although unilateral obstructive renal lesions are the most common form of urinary tract dilatation identified *in utero* with ultrasonography, one must be careful not to overlook the many other causes of nonobstructive hydronephrosis that occur in the neonate. Thus, thorough postnatal studies must be performed to confirm antenatal findings. Usually, the fetus seen to have hydronephrosis on prenatal screen is referred for postpartum ultrasonographic scanning to confirm the continued presence of hydronephrosis and for further evaluation. However, the infant should not be scanned too soon after birth since he/she will most likely be relatively dehydrated due to delivery and exhibit falsely negative results. Thus, it is suggested that the ultrasonographic study be obtained after adequate hydration and improvement in neonatal renal function, such as two to three weeks or more post partum, for the accurate assessment of hydronephrosis (2). In addition to postpartum evaluation, other indications for obtaining a diagnostic urinary sonogram in the pediatric population include renal or abdominal masses, or infections of the urinary tract.

Once hydronephrosis has been confirmed by ultrasonography, the next step is to differentiate between the obstructive and the nonobstructive causes of urinary tract dilatation. Currently, the diagnostic procedures used in the evaluation of hydronephrosis in children are achieved primarily through invasive means and include cystography, excretory urography with or without a diuretic, retrograde pyelography, renography with or without a diuretic, and pressure-perfusion studies (the Whitaker test) (3).

Vesicoureteral reflux as the cause of hydronephrosis is evaluated by two major methods, voiding cystourethrography (VCUG) and the radionuclide cystogram. The VCUG is the best anatomic test, for it clearly depicts the urethra, bladder, ureters, and kidney if reflux is present (4) and thus, should be the initial cystographic study when reflux is suspected. VCUG is usually performed in the evaluation of pediatric urinary tract infections. There are several ways to perform the VCUG including gravity filling of the bladder, hand injection of contrast into the bladder, and the suprapubic injection of contrast. In all three methods a 5 to 7.5 percent solution of organically bound iodine gives satisfactory contrast (5). With the first two methods, the patient is catheterized. The amount of the contrast placed into the bladder varies greatly since the goal is to completely fill the bladder so as to induce voiding (4). The patient is then turned so that a lateral or steep oblique position is assumed, and multiple radiographs are made of the urethra during the voiding process. After voiding is complete, an abdominal film is obtained to evaluate if there is any residual urine in the bladder and to see the presence of any reflux into the upper urinary tract that was not appreciated on fluoroscopy (5). Reflux may occur during filling, voiding or both. The degree of reflux should be determined and is divided into five grades of severity based on the degree of distention of the upper tract, specifically the ureters and fornices. However, one should realize that the severity of reflux can vary dramatically from one examination to another in a short period of time in

the same child. The fluoroscopy time and the number of radiographs taken during the study should be kept to a minimum, but should also show the maximum extent of the reflux, the vesicoureteral junctions and the urethra during voiding. At the end of the exam, the drainage of the renal pelvis and ureter should be assessed (6).

The radionuclide cystogram detects reflux with good sensitivity and requires a radiation dose of only one to two percent that of the radiographic VCUG. However, morphological detail is poor. The patient is catheterized and one millicurie of technetium-99m pertechnetate is placed into the bladder along with normal saline. With the patient in either the sitting or supine position (depending on age) the gamma camera is placed posteriorly and pictures are taken every 30 seconds. The patient subsequently voids around the catheter and pictures are obtained. Post-void residual volume is determined by the amount of radioisotope remaining in the bladder. Since imaging occurs continuously, the sensitivity of this study is high for the detection of significant reflux. However, since the bladder is filled with the isotope, visualization of small distal ureteral reflux, small ureteroceles or diverticula is not able to be accomplished (7). Since the radiation dose to the gonads is low, the radionuclide cystogram can be repeated relatively frequently and is the ideal method to follow the progress of known reflux in children managed conservatively (8).

The intravenous urogram was for many years the fundamental radiological examination of the urinary tract in children. It is now being challenged by other studies, but still retains a place as a useful mode of urinary tract imaging (9). The conventional excretory urogram can usually diagnose obstruction, but at times does not accurately differentiate between obstructive and nonobstructive hydronephrosis (3). The excretory urogram begins with a scout film of the abdomen to allow detection of calculi, to evaluate the spine and to assess the position and size of the viscera. Next, the injection of contrast

medium into a suitable vein is performed, which should take at least one minute to accomplish. After the injection, a 1-minute, coned-down prone radiograph of the kidneys called the nephrogram film is obtained, which shows the renal parenchyma quite well. Since the contrast media is filtered by the glomeruli and flows into the renal tubules, the axis, shape and size of the kidneys are readily determined on the nephrogram film. Contrast agents are entirely removed by glomerular filtration. By one hour, more than half of the injected dose is excreted and the goal of the subsequent films is to assess the collecting system and the ureters. Usually, films are obtained at 5- and 10- minute intervals after injection (10). Delayed views are obtained if there is a lack of visualization of the kidneys (11). In the neonate, the nephrogram is obtained at 3-5 minutes and the supine and lateral films are obtained at 10 to 20 minutes because of the lower renal blood flow, glomerular filtration rate and concentrating ability seen in the neonate. The fornices, calyces, infundibula and renal pelvis can be identified on the 5 minute and subsequent films. The ureters are often seen but not necessarily throughout their entire length in any one film. On the lateral views, the kidneys should overlies the vertebral bodies and the ureters course anteriorly along the psoas muscles. On frontal films, the ureterovesical junction can be seen and evaluated (10). Obstruction is manifested on excretory urography by prolonged filling of enlarged calyces, a delayed nephrogram, and collecting system dilatation proximal to the obstructed site. With severe, long-standing obstruction, no excretion may be detected (12).

Excretory urography can also be performed with the use of a diuretic based on the principle that with significant obstruction the urinary tract is unable to transport fluid over the physiologic range of flow rate and that diuresis produces an increase in the pelvicalyceal dimensions (3). After furosemide-induced diuresis, a 20 to 22 per cent increase in the area of the pelvicalyceal system has been reported to indicate significant

obstruction (13). Planimetry quantification of the changes in the size of the pelvicalyceal system is imprecise and this test is not reliable (3).

Retrograde pyelography is an imaging technique that is now rarely performed in children but is occasionally useful prior to pyeloplasty to confirm the normal caliber of the ureter, to clearly define suspected filling defects in the collecting system, and if other examinations are not available. The ureteric orifice is cannulated cystoscopically under general anesthesia and the catheter is moved up to the area of interest (14). Combining retrograde pyelography with fluoroscopy eliminates the disadvantage of blind filling and allows the ureteral catheter to be optimally positioned at the site of the suspected lesion. With the use of fluoroscopy, questionable obstruction to urine outflow in the upper urinary tract can be evaluated adequately (15).

The Whitaker test, or the percutaneous pressure perfusion test, is sometimes performed to distinguish a nonobstructed urinary system from an obstructed one. The upper urinary tract is perfused in an antegrade manner at a constant flow rate while the monitoring of the renal pelvic and bladder pressures is performed concurrently (16). If the ureter is obstructed, increasing the flow rate causes a significant rise in the pressure gradient. If the ureter is not obstructed the pressure gradient does not rise. The Whitaker test is performed by sedating the child with general anesthesia and inserting a bladder catheter, which is connected to a transducer or manometer. A percutaneous nephrostomy is performed under ultrasonographic guidance and the nephrostomy tube is connected to another pressure transducer or manometer. After baseline pressures are recorded, perfusion is started. In infants and small children, flow rates are started at 5 ml/min and in older children at 10 ml/min. Choosing the proper flow rate for different sizes of children renders this test controversial, since the pressure in an overtaxed system will rise. Contrast material can be injected into the nephrostomy tube and in so doing, the

functional characteristics of the ureter can be evaluated. A pressure gradient of less than 12 cm H₂O across the suspected obstruction that does not show a rise during infusion is considered normal. Obstruction results in a higher pressure, which rises to greater than 20 cm H₂O. A rise between 12 and 20 cm H₂O is equivocal (17).

Renal scintigraphy with diuretic renography has been considered the recent gold standard for the evaluation of function and drainage in hydronephrotic pediatric kidneys. Urinary tract dilatation without a demonstrable organic lesion is sometimes seen in children and the question of whether or not obstruction is present will inevitably arise. This dilemma has resulted in the wide acceptance of diuresis renography for the clarification of the hydronephrotic etiology. This study is based on the hypothesis that the truly obstructed dilated upper urinary tract will be obstructed at both low and high urine flow rates (18). On the other hand, the non-obstructed, yet dilated tract may appear obstructed at low flow rates due to a reservoir effect, but high flow rates induced by a diuretic will eliminate stasis and produce prompt washout from the upper tract (19). The technique used to perform diuresis renography is fairly simple. The child is first hydrated with intravenous fluid beginning 15 minutes before the injection of the radionuclide. He or she is then given an intravenous bolus of a radiopharmaceutical, usually 99m-technetium diethylene-triamine-pentoacetic acid (DTPA). This agent is excreted entirely by glomerular filtration, and the radiation dose to the kidney is the lowest of the commonly used isotopes (20). The patient is then positioned supine on the scanning table with the gamma camera underneath. An indwelling bladder catheter is inserted to ensure an empty bladder and a standard technetium-99 DTPA renal scan is performed. When the dilated collecting system is entirely filled with tracer, furosemide is injected intravenously. Sequential images and data are obtained for at least 30 minutes. Intravenous fluid is administered quickly during the first 30 minutes following furosemide injection, and the urine output during that time is measured. The computer

data are subsequently processed and the clearance half-time of the tracer from the upper urinary system is calculated. Studies have shown that most nonobstructed urinary systems drain with a half-time of less than 15 minutes, whereas most obstructed tracts either fail to drain or drain with a half-time of over 20 minutes. The range between 15 and 20 minutes is equivocal. However, the results are not reliable in the presence of poor renal function, extreme dilatation of the upper urinary tract, or poor response to furosemide (19).

The gamma camera renogram is comprised of a set of derived blood-background subtracted excretion curves and a series of images. The normal renogram curve demonstrates three classic phases. The first phase is the rapid rise immediately following the injection of the radionuclide which reflects the renal vascular supply. This subsequently gives way to the second phase, a more gradual slope which corresponds to the renal handling of the radionuclide as it is taken up by the kidney and passes through the collecting system of the nephrons. In the normal kidney, the curve then reaches a peak at 2-5 minutes and activity starts to leave the renal area, which marks the beginning of the third phase. The peak can be delayed by several different conditions such as obstruction preventing the excretion of tracer, renal artery stenosis causing a delayed supply of tracer to the kidneys, low urine flow rate or parenchymal disease. Thus, the third phase is predominantly excretory and is highly sensitive to abnormalities in the outflow tract so that a normal pattern excludes the presence of even trivial degrees of obstruction (21). Four basic responses to the diuretic challenge may occur (Figure 6). The first is the normal pattern which consists of spontaneous washout of the tracer (Group I). The second is the obstructed pattern which consists of progressive accumulation of the tracer in the dilated collecting system before furosemide injection with little or no washout after diuresis (Group II). The dilated, nonobstructed pattern consists of the gradual accumulation of tracer with prompt washout following the injection of furosemide

(Group IIIa). The fourth pattern is equivocal and shows an initial, gradual accumulation of the tracer with a minimal or moderate washout with the administration of furosemide (Group IIIb) (19). This pattern may indicate either a very mild degree of obstruction or a poorly functioning kidney that cannot effectively respond to the diuretic (22).

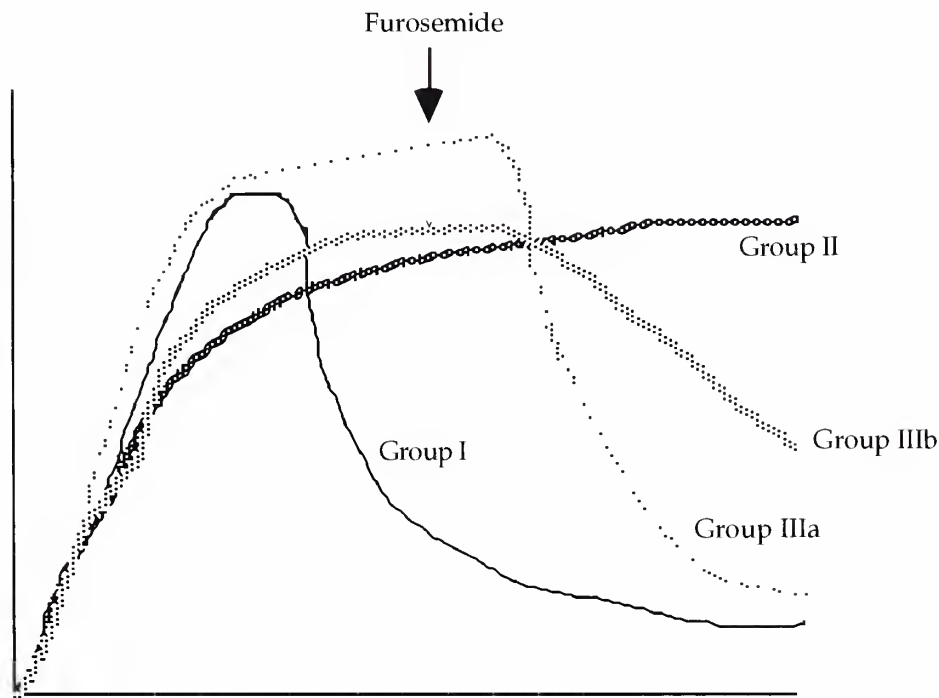


Figure 6. Diuresis renogram responses. (O' Reilly, Shields, R.A. and Testa, H.J. *Nuclear Medicine in Urology and Nephrology*, 1986, p.97).

Even if the diagnosis of urinary tract obstruction is straightforward, the percentage of function in each kidney is important information in patient care. A useful method to determine relative renal function is to evaluate the mean radionuclide uptake for each kidney by the calculation of the area under each background-corrected renogram between 1 minute after injection and at either 3 minutes, or 20 seconds before the first peak,

whichever occurs earlier. The individual renal function is consequently expressed in percentage terms as the ratio of the mean uptake for each kidney to the sum of the two (21).

As one can intuitively surmise, the major limitation to the diuretic radionuclide urogram is depressed renal function which may invalidate the results (23). Also, children under one month of age demonstrate incomplete renal maturation, and so the effects of diuretics are less predictable. Thus, a flat excretion curve under these circumstances may indicate either obstruction or poor renal function (24). Other shortcomings to the procedure include its expense, its use of ionizing radiation, its 10-15% rate of false positive and indeterminate results, and its need for an intravenous line and bladder catheterization (25).

DIAGNOSIS OF URINARY TRACT OBSTRUCTION BY SONOGRAPHY IN THE PEDIATRIC PATIENT

Ultrasonography is a noncontrast tomographic study that usually does not require any special patient preparation or sedation (1). Sonographic imaging is not dependent on organ function; thus, the functionally impaired kidney can still be effectively delineated. The examination is extremely flexible as scanning can be accomplished in multiple planes and with the patient in almost any position in any location. Its use in the pediatric patient is ideal because it is painless, lacks known risk, injections, and ionizing radiation, and it allows parents to remain close to their children (2). Additionally, the pediatric patient is ideally suited for ultrasound, for small size and relative lack of body fat facilitates scanning (3).

To better understand the specific appearance of the abnormal, obstructed kidney and urinary tract on sonography in the pediatric patient, that of the normal kidney and collecting system must first be discussed. As mentioned previously, it is known that different organs have characteristic textures. The absolute intensity, or echogenicity, of a particular organ will be relatively constant, thus allowing the diagnosis of abnormality (4). Those organs with a fairly uniform composition of the parenchyma, such as the liver and the spleen, produce a relatively homogeneous echogenicity and thus, provide very good references for examining the kidneys (5). The renal cortex is normally less echogenic than the normal liver and spleen (Figure 7).



Figure 7. Echogenicity of the kidney. The echogenicity of the normal kidney is demonstrated in this supine longitudinal right upper-quadrant scan. Note the lower echogenicity of the kidney as compared to that of the normal homogenous liver (arrow).

However, in the neonate this echogenic difference is much less marked. With ultrasonography, the renal capsule, cortex, medulla, and the renal sinus can all be identified quite clearly. The renal sinus consists of the calyces, infundibula, pelvis,

arteries, veins and fat ultrasonographically and thus, is intensely echogenic, or hyperechoic (Figure 8). This region is normally collapsed, but during periods of diuresis, may show considerable distention.

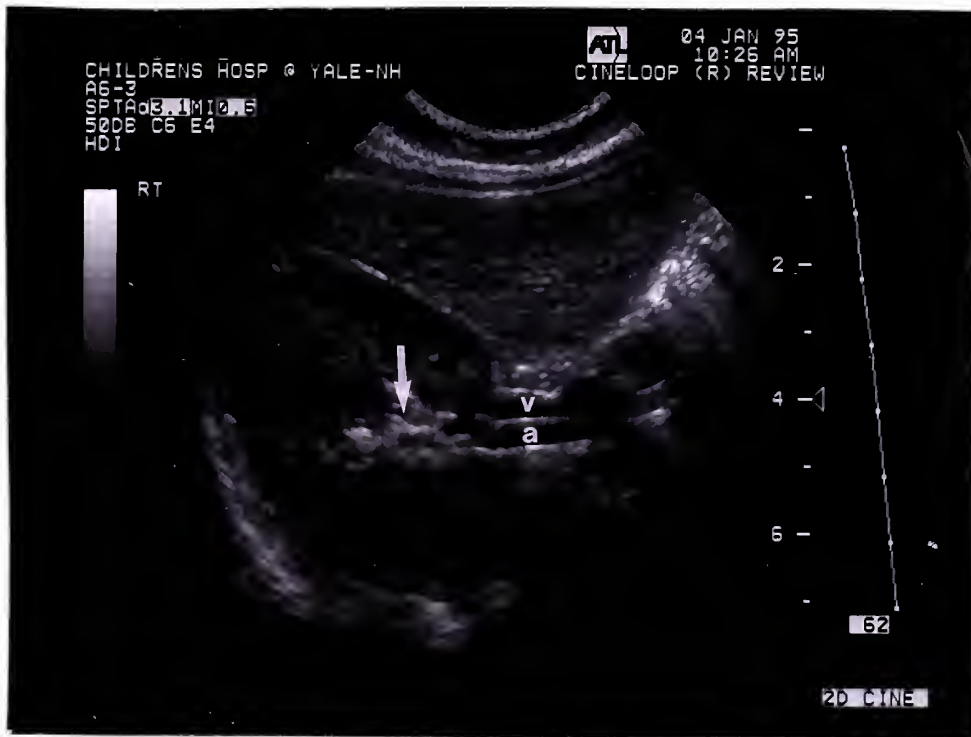


Figure 8. The hyperechoic renal sinus. Dense echoes formed by the renal sinus are demonstrated in this transverse scan (arrow). In addition, the renal artery (a) and vein (v) can be seen clearly entering the hilum of the kidney.

Within the parenchyma, the cortex and the columns of Bertin show greater echogenicity than the medulla, where the individual renal pyramids form round or triangular areas of low echogenicity. At the margins of the cortex and the medulla, the arcuate arteries can be seen as small, intense echogenic foci (5) (Figure 9).



Figure 9. The increased echogenicity of the renal cortex. The difference in echogenicity between the renal medulla and cortex is shown. The prominent rounded areas of low echogenicity formed by the individual renal pyramids are demonstrated (arrow). Also, foci of increased echogenicity from the arcuate arteries can be demonstrated at the margins of the cortex and the medulla.

There are significant differences in the normal sonographic findings with age (Figure 10). In neonates, the kidneys are relatively quite large, their length ranging from 3.3-5.0 cm, the width from 2-3cm and the diameter from 1.5-2.5 cm (6). Fetal lobulation may also be prominent. The echogenicity of the renal cortex approaches that of the liver and spleen, so that the renal outline is less clearly defined in neonates (5). The increased echogenicity in the neonate may be related to several factors: the greater volume that the glomeruli occupy in the cortex (19% in infants vs. 9% in adults); the thinner glomerular basement membrane in adults; the greater number of loops of Henle in the neonatal cortex, and the surrounding of infant glomeruli by a cuboid epithelium (7). This neonatal

pattern of echogenicity changes to adult pattern of decreased echogenicity of the renal cortex between 2 and 3 months of age, with 90% taking on the adult appearance by age 4 months (8). However, the most striking feature of the normal neonatal kidney is the prominence of the medullary pyramids which are quite large in size and appear almost anechoic. Thus, these pyramids can be mistaken by the inexperienced for hydronephrosis or cysts. In infants, the presence of fat, which is a highly echogenic substance, is not a significant feature in the renal sinus and surrounding fascia, and result in a less distinguishable renal sinus (5).



Figure 10. The neonatal kidney. Prominent fetal lobulations are seen in this neonate's kidney. The increased echogenicity of the normal neonatal kidney makes its differentiation from the normal liver more difficult (arrow). Note also the large size of the medullary pyramids, which appear to extend almost to the renal periphery and may be mistaken for cysts or hydronephrosis.

Because of their small diameter of approximately 5 mm, the normal ureters are not usually visualized sonographically. Even when the ureter is dilated, much of its mid-

portion is often hidden by gas in the bowel and only the upper and lower few centimeters are visualized. However, a dilated fluid-filled ureter can usually be traced down to its insertion in the posterior aspect of the bladder. The presence of normal peristaltic waves as well as any confusion with pelvic vessels can be resolved by real-time imaging, which also offers a third advantage of observing increasing ureteral dilatation during and after voiding if vesicoureteral reflux is present. (9).

The bladder is an ideally suited structure for sonographic imaging since it is often distended with urine. When distended, the bladder assumes a trapezoidal shape on the transverse supine sonogram (9). The bladder wall normally appears as a smooth, symmetrical, curved surface. Bladder wall thickness can be determined with sonography as well as bladder volume and residual urine volume (10). Real-time sonography allows the visualization of the urine as it enters the bladder from the ureters, as well as the vesicoureteral reflux of urine at times (11).

As mentioned previously, obstruction is detected by ultrasound based on the dilation of the collecting system. The ultrasound appearance of hydronephrosis depends on the degree of calyceal and renal pelvic dilatation. In mild hydronephrosis, the central echo complex appears separated by a large, anechoic pelvis that communicates with dilated calyces and the cortex remain intact (12) (Figure 11). As the obstruction progresses, the fluid-containing region becomes larger and the dilated calyces are seen in the periphery of the renal sinus. Actually, when the entire renal pelvis is seen together with the calyces, the findings resemble the ears and face of Mickey Mouse. In massive distention, separation of the calyces and pelvis may actually be lost. In all but the mildest degrees of hydronephrosis, the renal parenchymal rim will be reduced in thickness in the presence of obstruction. In extreme cases, the collecting system is so distended that the parenchyma is reduced to a thin sliver overlying stretched out calyces (13) (Figure 12).



Figure 11. Mild hydronephrosis. Minimal fullness of the renal pelvis without infundibular or calyceal enlargement is demonstrated in this sonogram. The renal cortex remains intact with no parenchymal thinning noted.

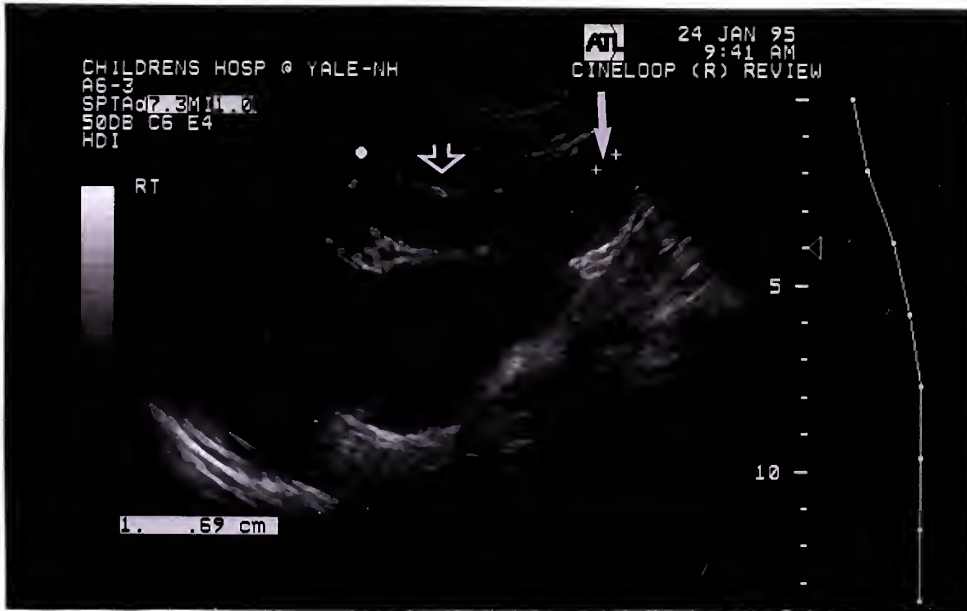


Figure 12. Severe hydronephrosis. This poorly functioning kidney showed an outpouched hydronephrotic sac with a thinned parenchymal rim measuring 0.69 centimeters (long arrow). Also seen is the increased echogenicity of the atrophied parenchymal rim compared to that of the normal liver (arrowhead).

Several other morphological indices in the urinary tract have been found to be present sonographically in patients with obstruction. In obstruction with moderate to severe hydronephrosis, varying degrees of cortical atrophy can be detected, which appears sonographically as increased echogenicity of the thinned parenchyma (Figure 12). This was demonstrated in a recent study by Crumbleholme et al (14) in which all eight patients studied who displayed increased echogenicity on sonography, were found to have underlying renal dysplasia. Other variables that can be assessed in regards to urinary tract obstruction include the size of the obstructed kidney as well as the presence of compensatory hypertrophy of the contralateral kidney. The kidney which is acutely obstructed initially enlarges as a result of both distention of the calyces and parenchymal edema. As the renal blood flow begins to fall, the calyces partially regress to be followed by the progressive atrophy of the tubules (15). Compensatory hypertrophy has been shown to occur in a normal kidney when the other has been removed, fails to develop, or is destroyed by disease, such as obstructive nephropathy (Figure 13). The degree of compensatory hypertrophy is greatest in younger patients (16). Laufer and Griscom found that 66% of the contralateral hypertrophy occurs within 2 months of the insult and it is usually complete by one year (17).



Figure 13. Compensatory hypertrophy. This patient possessed a poorly functioning contralateral right kidney. The left kidney (shown here) demonstrates compensatory hypertrophy measuring 13.0 cm, two standard deviations above the mean for a patient of his age. On further radionuclide examination, it was shown that this kidney provided 85% of the total renal function for this patient.

Hydronephrosis of only a portion of the kidney may be seen sonographically and usually indicates obstruction of the upper collecting system of a duplex kidney. In obstruction of a duplicated kidney, the dilated ureter of the upper segment will be seen medial to the lower segment of the kidney. Ureterocele are commonly present in these patients and sonographically can be seen as a cystic mass protruding into the posterior bladder (18).

If bilateral hydroureteronephrosis is detected in the male infant, posterior urethral valves must be considered. The simultaneous observation of both dilated ureters can be

achieved by transverse scanning over the distended bladder. Associated findings of bladder wall thickening and trabeculation as well as dilatation of the prostatic urethra can be demonstrated (12).

The most common site of obstruction is the ureteropelvic junction, but when obstruction occurs more distally, a dilated ureter will be seen running down from the renal pelvis (13). A dilated ureter is seen as a tubular, fluid-filled structure which extends caudad along the medial aspect of the kidney and on the psoas muscle (Figure 14). However, a markedly tortuous ureter may not be imaged as a long, tubular structure, but as a series of ovoid, fluid-filled spaces (18). Careful examination of the ureter may demonstrate the extrarenal cause of the hydronephrosis, such as a calculus (17). When dilated ureters are seen posterior to the bladder, obstruction at or below the ureterovesical junction should be considered. However, this can also be the result of vesicoureteral reflux (12).

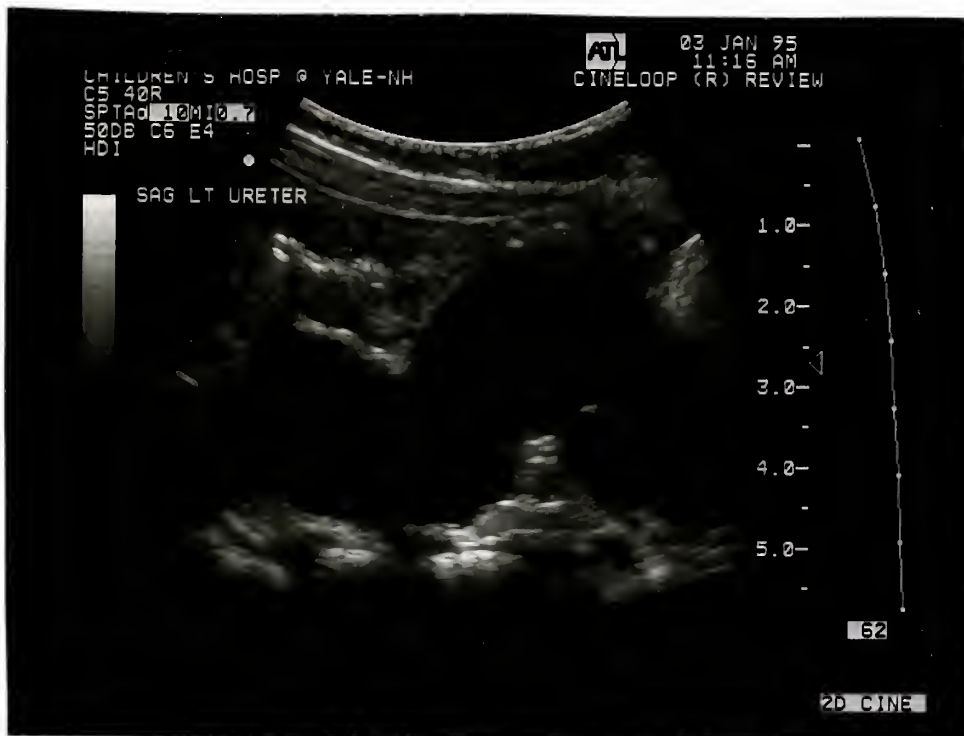


Figure 14. A massively dilated ureter. This left sagittal sonogram demonstrates an obstructed, tortuous ureter measuring 2.33 centimeters in width. The normal ureter is almost never visualized sonographically.

In the presence of obstruction, the ureteral pressure and subsequently, its dimensions, including length and diameter, increase. These dimensional changes are manifested sonographically by ureteral dilatation and tortuosity (Figure 14). This increase in baseline intraluminal pressure depends upon the continued production of urine by the kidney, which cannot pass freely beyond the level of obstruction. In turn, the increase in ureteral dimensions is a consequence of the increased ureteral luminal pressure and the increase in the urine volume which is retained in the ureter. A few hours after obstruction has taken place, the intraluminal ureteral pressure reaches a peak and then begins to decline. However, the increased dimensions of the ureter remain stable due to the hysteretic properties of the viscoelastic structure of the ureter. In addition, as the obstruction persists over time, the ureteral length and diameter continue to increase even in the face of this relatively low intramural pressure. This phenomenon can also be explained by the viscoelastic ureteral structure. Unfortunately, ureteral dilation may also occur secondarily to vesicoureteral reflux or as a primary process without the presence of either reflux or obstruction (19). This makes the sonographic imaging of an increase in ureteral diameter a rather nonspecific finding.

The functional capabilities of sonography can also be quite useful in distinguishing obstructive from nonobstructive hydronephrosis in children. As discussed in a previous section, ureteral peristalsis can be detected with the use of real-time sonography. Normally, urine is conducted from the kidney to the bladder by ureteral peristaltic waves, occurring at a rate of 2 to 6 contractions per minute. However, in cases of acute ureteral obstruction, the increase in intraureteral pressure causes peristalsis to gradually cease. Fortunately, the absence of peristalsis seems to be a phenomenon specific to obstruction and hence, can be a useful marker for identifying obstructive processes sonographically (20). For example, although a decrease in peristaltic frequency

is observed in high grade reflux, with bacterial toxins and with several antibiotics, the absence of peristalsis is not demonstrated (21, 22, 23). The utility of sonographically identifying the absence or presence of peristalsis in the diagnosis of obstruction was recently studied by Keller et al (20), in which they demonstrated that when a dilated, aperistaltic ureter is imaged by sonography, the presence of severe obstruction or poor renal function is highly implied, with a sensitivity of 81% and a specificity of 100%. Conversely, when a dilated, peristaltic ureter is seen, vesicoureteral reflux is the most likely cause and obstruction can be excluded with a specificity of 93% . While the presence of peristalsis can be detected in some obstructed ureters, the obstruction is most likely not of a severe nature (20).

Although ultrasonography has attained a prominent role in the detection of hydronephrosis in fetuses, infants and children, its use in the differentiation between the obstructive and nonobstructive etiologies of dilated collecting systems has been highly criticized, being labeled as a highly sensitive, yet nonspecific detector of dilatation of the collecting system (24). Since the extent of hydronephrosis depends on several factors such as duration of obstruction, completeness of obstruction, compliance of renal parenchyma, state of hydration and renal function, many false-positive and false-negative causes of hydronephrosis can lead to an inaccurate sonographic diagnosis of obstruction in children. Potential causes for false-positive sonograms include: a large extrarenal pelvis, high urine output states, nonobstructive dilatation of the collecting system, congenital megacalyces, reflux nephropathy, severe papillary necrosis and parapelvic cysts. Conversely, possible causes for false-negative sonographic imaging include: the presence of a calculus, blood clot , or pus in the pelvicalyceal system (24), an early stage of obstruction, partial or intermittent obstruction, a decompressed pelvicalyceal system, retroperitoneal fibrosis, hypovolemia or dehydration, severe parenchymal disease or a scarred kidney (25, 26). However, further refinements in

sonography have produced enhanced anatomic delineation and have added the capability to demonstrate renal artery waveform analysis by duplex Doppler techniques (2). This has resulted in the emergence of many investigations performed to delineate the clinical applications of ultrasonography in the differentiation of hydronephrosis in children.

In 1979, Arima et al. identified an alteration in renal arterial blood flow patterns in transplanted kidneys undergoing rejection using Doppler ultrasound (27). This alteration was seen in association with an increase in renal arterial resistance, which resulted from a decrease in diastolic blood flow greater than the decrease in systolic flow. The relative variation of blood flow has been quantified by the resistive index $[RI = (\text{peak systolic velocity} - \text{lowest diastolic velocity}) / \text{peak systolic velocity}]$ (28), which has been described in a previous section. This elevation in the resistive index reflects the increased interstitial pressure of the affected kidney rather than a hormonal response (29). The use of resistive indices began in 1982, when Berland et al. evaluated the intrarenal vasculature of the transplanted kidney to detect rejection (30). Then, in 1987, Rifkin et al. identified criteria for diagnosing acute rejection of renal allografts based on the measurement of renal resistive indices (31). Since that time, urinary obstruction has been shown to cause an increase in the vascular resistance in the kidney and a decrease in renal perfusion that persists throughout the period of obstruction in animal models (32, 33).

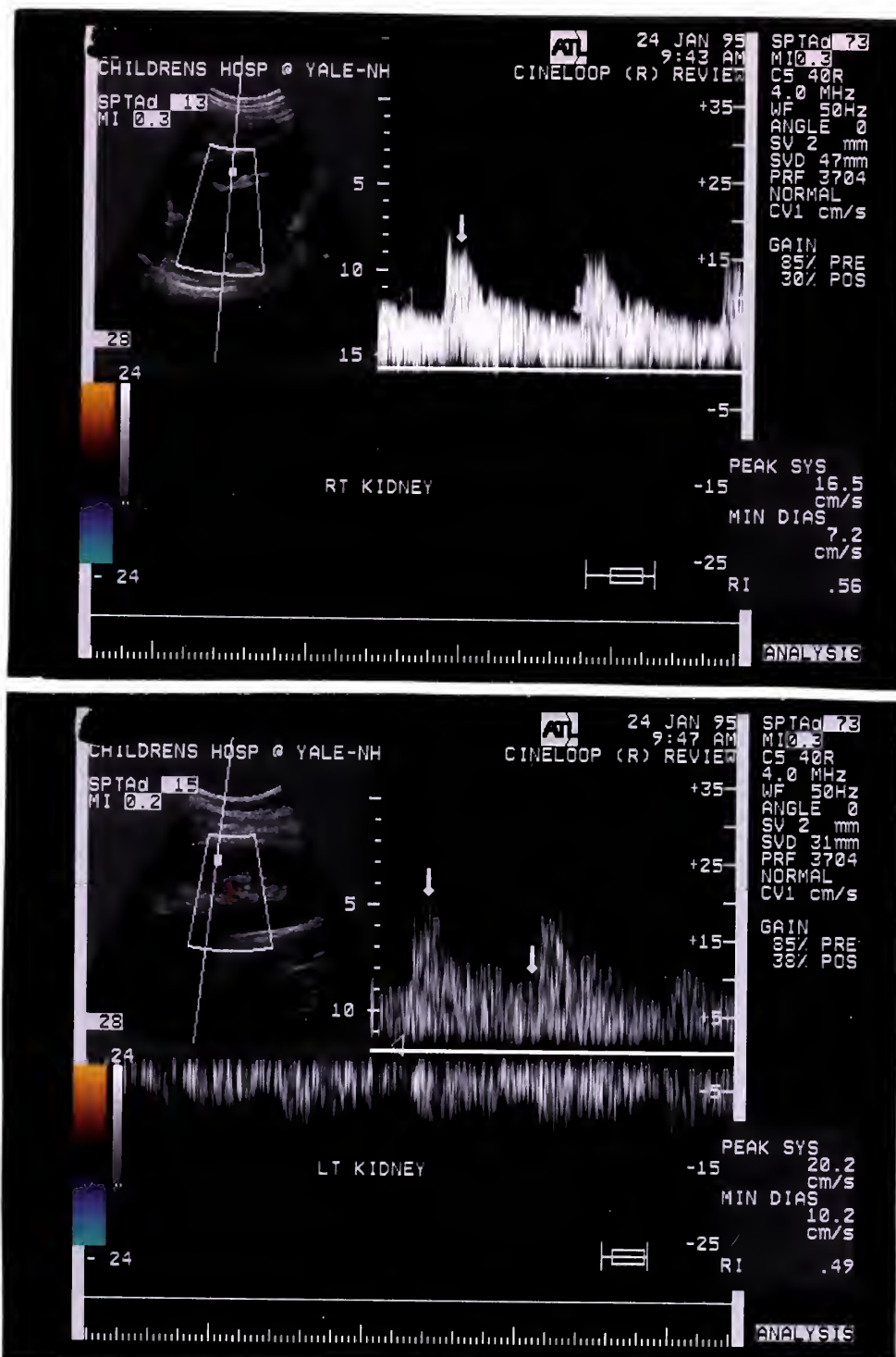
Based on this research in animals, Doppler techniques have recently been used to determine the resistive indices of hydronephrotic kidneys in humans. This began with a study by Platt et al. in 1989 (34), in which elevated renal resistive indices (greater than 0.70) were discovered in 13 of 14 obstructed kidneys immediately before percutaneous nephrostomy with a sensitivity of 92% and a specificity of 88%. Since then, others have also reported high renal resistive indices in adults seen in the presence of urinary tract obstruction (35, 36, 37, 38).

In 1991, Dodd et al. (39) used a canine model to examine the reproducibility of the above resistive index calculation in urinary tract obstruction. The left ureter of 5 dogs was ligated with suture and the remaining 6 dogs constituted the control group. Using the discriminatory RI variable of 0.7 to differentiate obstructive from nonobstructive hydronephrosis, they observed an overall sensitivity of 74% and specificity of 77%, with a false positive rate and false negative rate of 23% and 26%, respectively. Of perhaps greater interest, Dodd also found that the rise in the value of the resistive index was detectable as early as 24 hours after obstruction. These findings led the authors to caution against the use of Doppler sonography as a screening test for urinary tract obstruction. However, this lack of elevation of the resistive index could be caused by a decrease in the absolute blood flow in chronic, high-grade obstruction, decreased filtration pressure due to a minimally functioning renal cortex, the elevated compliance in a dilated, capacious collecting system, or due to failure of the dog model (40).

Unfortunately, the use of an absolute resistive index value in evaluating obstruction can not be extrapolated to the pediatric population. Although a study by Kessler et al. (41) demonstrated the resistive index of 0.70 as an effective cutoff for the differentiation of hydronephrosis in 30 children, most other studies have shown that the resistive index is an age-dependent parameter. In 1989, Wong et al. examined the Doppler waveforms in the interlobar arteries of 38 healthy children up to 12 years of age. They reported a mean RI of 0.76 ± 0.07 in children aged 0-2 weeks, 0.77 ± 0.08 in children aged 2 weeks to one year, and 0.68 ± 0.06 in children aged one to 12 years (42). In 1990, Keller et al. reported the resistive indices measured in segmental renal arteries in 25 children. They found RIs of 0.8-1.0 in premature infants, 0.6-0.8 in neonates, infants and toddlers, and 0.55-0.75 in preschool children. Above the age of 5 years, RIs were found to be 0.50-0.70 and thus, became independent of age (43). In 1992, Bude et al. (44)

also examined the age-dependency of RIs in children and discovered similar results to Keller et al.'s data, with the exception of preschool children, where they found the range of RIs to be between 0.54-0.72. In addition, Bude et al. concluded that adult mean RI criteria is applicable to children aged 4 years and older. Lastly, in 1993, Gilbert et al (45) demonstrated that in control pediatric kidneys, significantly different resistive index values were noted between patients 0-12 months old, who had an average RI of 0.66, and patients older than one year of age, with an average RI of 0.57. They also showed that renal units with obstructive hydronephrosis had RI values that were significantly higher (0.83 ± 0.095) than those with nonobstructive hydronephrosis (0.63 ± 0.053).

In an attempt to circumvent this age dependency, Keller et al. in 1991, formulated a new value, the resistive index ratio (RIR) and investigated its use (46). The RIR is defined as the ratio of the resistive index of the obstructed kidney to the normal kidney (Figures 15 and 16). In the control patients, the RIR is defined as the ratio of the resistive index of the right kidney over that of the left. They found the mean RIR in normal kidneys to be 1.00 ± 0.05 , the mean of dilated, non-obstructed kidneys to be 1.01 ± 0.05 and that of dilated, obstructed kidneys as being 1.16 ± 0.12 , with a sensitivity of either no detectable signal or an $RIR \geq 1.11$ for detecting obstruction of 77% and a specificity of $RIR \leq 1.10$ for excluding obstruction of 81%. Thus, this work defined criteria in a population in which age-dependent variations in renal blood flow must otherwise be considered (40).



Figures 15 and 16. The resistive index ratio. The inset figures show the area sampled for determining the resistive index. The arrows indicate the highest systolic and lowest diastolic values for each kidney. From these values, the resistive index is calculated. The resistive index of this patient's dilated right kidney was determined to be 0.56 and that of his normal left kidney was 0.49. Thus, the resistive index ratio was calculated to be 1.14, a value which implies obstruction of the hydronephrotic right urinary tract.

Unfortunately, the use of the resistive index ratio is dependent upon a normal contralateral kidney as a control and hence, it is not applicable in patients with a solitary kidney or possessing bilateral obstruction. However, recently, the pursuit of an alternative approach for the Doppler sonographic evaluation of obstruction in children has been undertaken, with the evaluation of the resistive index before and after furosemide administration. Palmer et al. (47) and Keller et al. (48) both recently investigated this phenomenon and both showed that furosemide diuresis increases the resistive index above baseline in obstructed kidneys; however, in Palmer's study, the resistive index increase above the prediuretic state was not statistically significant using a nonparametric test. However, Bude et al. reanalyzed Palmer's data on a normal distribution, and consequently found a statistically significant increase in the resistive index 10 minutes after furosemide in obstructed kidneys. However, at 30 minutes, the elevation was no longer statistically significant (44). Keller et al. reported that in obstructed kidneys, a mean increase of 11% (range 7-16%) was seen in the resistive indices after furosemide administration and concluded that the provocation of the RI to increase 10-15% or greater appears to support the diagnosis of obstruction. In addition, both studies showed that furosemide did not significantly affect the resistive index in normal kidneys as well as nonobstructed hydronephrotic kidneys when comparing baseline RIs with those obtained 10 minutes (48) or 10 and 30 minutes (47) after furosemide injection. Also, in adults, a third study by Renowden and Cochlin (49), scanning before and 10 minutes after furosemide, demonstrated that furosemide does not affect the resistive index of normal kidneys and causes the RI in obstructed kidneys to increase above baseline. Thus, with diuretic Doppler sonography, the individual renal units act as their own controls and thus, is quite applicable in the presence of a solitary kidney or of bilateral urinary tract obstruction.

However, in a recent abstract by Patriquin et al. (50), the RI difference in the presence of furosemide as well as the RIR were unable to significantly distinguish obstructive hydronephrosis from nonobstructive hydronephrosis in 45 children and thus, potentially questions the use of these measurements, although this is presently the only study in which the RIR and RI difference were not successful in the differentiation of hydronephrosis in children.

Also in 1994, Bude et al. (51) added to the concept of diuretic Doppler sonography by evaluating the effect upon the resistive index of the administration of an intravenous normal saline fluid load to diuretic-challenged nonobstructed kidneys to determine whether or not this caused any significant additional change in the resistive index that would aid in the evaluation of hydronephrosis. Eight children were given a fluid load of 12 cc of 0.9% sodium chloride per kilogram infused during a 30 to 60 minute interval followed by the administration of furosemide. The researchers found that the mean resistive index significantly decreased from baseline by a mean of 0.06 ± 0.06 and concluded that the significant resistive index decrease was the result of the combination of the fluid load and the furosemide, since in previous studies, a significant decrease has not been appreciated with furosemide alone (47, 48, 49). Hence, the addition of an intravenous fluid-load in addition to a diuretic appears to be more accurate in the evaluation of potentially obstructive hydronephrosis in children in whom a simple resistive index threshold of 0.70 does not apply.

In conclusion, a variety of different parameters have been investigated to date that attempt to sonographically differentiate obstructive from nonobstructive hydronephrosis in the pediatric patient. Each prognosticator has its own specific value in the distinction of hydronephrosis. However, the evaluation of all of these morphologic as well as

functional variables by sonography has yet to be undertaken in a single clinical study.

The remainder of this work is dedicated to achieving this task.

PURPOSE

Prior studies have focused on single sonographic parameters to differentiate obstructive from nonobstructive hydronephrosis in children. The primary purpose of this study was to identify ultrasonographic prognostic indicators to aid in distinguishing these two entities. This study begins with the investigation of the diagnostic utility of several independent parameters in the differentiation of hydronephrosis in children as compared against the standards of the diuretic radionuclide renogram as well as other invasive urographic examinations.

A secondary purpose was to develop a clinical scoring system using those indicators deemed significant in order to sonographically predict which children are at a greater risk for having urinary tract obstruction and thus, to obviate the need for further, more invasive diagnostic modalities.

MATERIALS AND METHODS

The ultrasonographic and other diagnostic radiographic evaluations of 635 renal units performed between January, 1992 and November, 1994, at the Yale-New Haven Hospital Department of Pediatric Diagnostic Imaging were retrospectively reviewed. The study group consisted of 320 children of whom 56 had normal kidneys, 154 had unilateral collecting system dilatation and a contralateral normal kidney, and 110 possessed bilateral renal collecting system dilatation.

Children who were suspected of having urinary tract obstruction following a diagnosis of hydronephrosis by sonography, either on prenatal screening or due to clinical symptomatology, underwent a series of examinations which consisted of a baseline sonographic study, Doppler sonography and diuretic Doppler sonography (performed by Drs. Marc S. Keller, Holly Korsvik, Dana Schwartz or Marcelle Piccolello). In addition, voiding cystourethography was also performed in the majority of the subjects to evaluate for vesicoureteral reflux. Due to the nature of a retrospective study, all of the subjects did not undergo all of the aforementioned radiological examinations. Thus, only if obstruction remained a likely cause for the hydronephrosis detected by sonography did the subjects undergo further radiographic or radionuclide excretory studies (performed by Drs. Paul Hoffer, Eugene Cornelius, or Holley Dey in the Department of Nuclear Medicine). If a patient had more than one examination of a particular type performed, those imaging studies that were the closest temporally related were included in the data.

Twelve ultrasonographic variables were chosen to be examined in this study. However, many of the patients did not have complete data sets and the number of renal units analyzed for each parameter varied (Table 1). The sonographic parameters which

were evaluated were those which had been previously examined by other authors and included: the resistive index (1, 2, 3, 4), the post- diuretic resistive index (5, 6, 7, 8), the difference in the resistive indices pre- and post- diuretic (5, 6, 7, 8), the resistive index ratio (7, 9), and the presence or absence of peristalsis (10); as well as several other variables from published observations and clinical experience which were never before evaluated, yet suspected of being valuable predictors for differentiating obstructive from nonobstructive hydronephrosis. These included: the dimensions of the ureteral diameter (11), the size of the hydronephrotic kidney (12), the presence of contralateral hypertrophy (13), the echogenicity of the kidney (14), the dimensions of the parenchymal rims (15), the post-diuretic resistive index ratio, and the difference in RIR pre- and post-diuretic.

TABLE 1

VARIABLE	RENAL UNITS
Resistive Index	288
Resistive Index after diuretic	112
Resistive Index difference with diuretic	112
Resistive Index Ratio	147
Resistive Index Ratio after diuretic	54
Resistive Index Ratio difference with diuretic	54
Ureter diameter	635
Presence or absence of peristalsis	635
Kidney size	635
Contralateral hypertrophy	635
Echogenicity	635
Parenchymal rims	635

All of the sonographic examinations were performed using an ATL Ultramark 5, Ultramark 9 (Advanced Technology Laboratories, Bothell, WA) or Acuson 128 unit (Elmwood Park, New Jersey) using 3.5, 5 or 7.5 MHz frequencies on a phased-array transducer by the aforementioned physicians. No sedation was employed during the examination. The children were neither fluid-restricted nor intentionally hydrated before the examination. Renal morphology was studied in both the longitudinal and transverse planes for assessment of size of the kidney, pelvicalyceal dilatation, echogenicity, the dimensions of the parenchymal rims, the presence of calculi, or any other morphological abnormality. When one renal unit was found to have some degree of hydronephrosis, the opposite kidney, if present, was always examined to evaluate for contralateral hypertrophy.

Ureteral dilatation was defined as a sonographically identifiable fluid-filled ureteral lumen. The diameter of the ureter was measured at the most distal portion that could be visualized. Real-time observation was performed for a minimum of one minute to determine the presence or absence of ureteral peristalsis. Peristalsis was defined as the segmental coaptations of the ureteral walls which moved in a craniocaudal direction, and were always imaged in longitudinal and transverse planes in all instances.

Pulsed Doppler spectra were obtained by examining the area of the corticomedullary junction with a Doppler probe. Once the localization of the segmental or interlobar arteries was accomplished by color flow Doppler sonography, the resistive indices were measured from the formula: $(\text{peak systolic velocity} - \text{end diastolic velocity}) / \text{peak systolic velocity}$ and were calculated using the built-in software. The measured resistive indices of two to three equivalent-appearing waveforms taken from the upper, middle and lower poles of each kidney were averaged in order to obtain a mean resistive

index. When possible, the patient's opposite kidney was used as a control and the resistive index ratio was obtained as the ratio of the RI of the obstructed kidney over that of the nonobstructed kidney. In those patients identified as having normal renal units by baseline sonography, the RIR was defined as the ratio of the RI of the right kidney over that of the left. If it was clinically indicated, following the baseline sonographic study, each subject was given 0.5 mg/kg of furosemide along with a fluid bolus of 15 mg/kg intravenously. At approximately 10 minutes after injection of the diuretic, the resistive indices and resistive index ratios were again measured using the same methodology as described above.

The diuretic radionuclide renograms were obtained in those children who, on the basis of sonography, continued to be suspect for having urinary tract obstruction. The standardized approach as described by Majd (16) was utilized for performing the diuretic renal scans. All of the patients were intravenously hydrated with 5% dextrose in 0.3% sodium chloride (15cc/kg) beginning 15 minutes before the injection of the radionuclide. An indwelling bladder catheter was inserted to maintain an empty bladder as well as to monitor urine output during the study. Two and one-half $\mu\text{Ci}/\text{kg}$ of the radionuclide $^{99\text{m}}\text{Tc}$ DTPA, was administered as an intravenous bolus. Renal function was measured by rapid sequence 10-second posterior projection images. When the radionuclide activity in the hydronephrotic kidney and the renal pelves began to peak, 0.5 mg/kg furosemide along with a fluid bolus of 15 mg/kg were intravenously administered and the timed excretion was observed. The data were collected at 30 second intervals for 40 minutes into a computer matrix size of 64 X 64 X 16 bits. Acquisition time was one minute. Selected regions of interest were drawn and time/activity curves were generated and displayed for each renal unit. A quantitative analysis of the amount of time taken for half of the isotope to wash out of the collecting system (half-time) was calculated. Relative renal function was calculated from the integral of the background. The ability to respond

to the diuretic was measured by measuring the urine output from the bladder catheter before and after the intravenous injection of furosemide. An abnormal diuretic radionuclide renogram indicative of obstruction was one in which the half-time clearance of the radionuclide after furosemide administration was greater than 20 minutes.

The assignment of a final diagnosis was determined not only by the diuretic radionuclide renogram as described above, but also by several other radiographic examinations, such as the voiding cystourethrogram and the excretory urogram, according to the well-established standardized methodology. If vesicoureteral reflux into the upper collecting system was demonstrated on voiding cystourethrography followed by immediate drainage into the bladder on post-voiding radiographs, nonobstructed reflux was diagnosed. The demonstration of posterior urethral valves by voiding cystourethrography was classified as obstruction. The kidneys were considered obstructed when the excretory urogram demonstrated a delayed appearance of the pyelogram without the passage of contrast material below the obstructed site. When the excretory urogram demonstrated complete renal duplication with upper pole hydroureteronephrosis and delayed contrast medium excretion, obstruction was also diagnosed. Those cases with hydroureteronephrosis terminating in an ectopic ureterocele studied by excretory urography were considered to have obstruction. In those children with sonographically visible hydronephrosis where neither diuretic radionuclide renography nor voiding cystourethrography or excretory urography showed any abnormality were classified as nonobstructed.

DATA COLLECTION

The pediatric urologist at Yale-New Haven Hospital, Dr. Robert M. Weiss, provided a list of all of his patients who were diagnostically labeled as having either "hydronephrosis" or "evaluate for obstruction". The ultrasonographic and other diagnostic radiographic reports of these patients were obtained by using the DEC-RAD computerized reporting system in the Department of Diagnostic Imaging. Pertinent radiographic information from each report was recorded on data collection forms and was entered on a spreadsheet using the Macintosh Microsoft Excel© computer software. Subsequently, this data was entered into the Statistical Analysis Software© database in the Yale University Department of Epidemiology and Biostatistics and the necessary statistical comparisons were calculated using this software.

DEVELOPMENT OF THE HYDRONEPHROTIC OBSTRUCTIVE SCORING SYSTEM

The renal units were classified into three major groups: 1) normal kidneys without evidence of obstruction, vesicoureteral reflux, or any other abnormality, 2) hydronephrotic nonobstructed kidneys, and 3) hydronephrotic obstructed kidneys. For the purpose of statistical analyses, those renal units classified as normal and those labeled as hydronephrotic and nonobstructed were categorized as nonobstructed and hence, the presence or absence of obstruction was evaluated as a dichotomous variable.

The following entities were also evaluated as dichotomous variables: absence of peristalsis, size of kidneys, presence of hydronephrosis, contralateral hypertrophy, and echogenicity. Variables which were initially submitted as continuous variables, but turned out to be better predictors as dichotomous variables included: ureteral diameter,

pre and post-diuretic difference in resistive index, the resistive index ratio, the post-diuretic resistive index ratio, the difference in resistive index ratio pre and post diuretic, and the length of the parenchymal rims.

Cutoff criteria for the presence of urinary tract obstruction chosen for each ultrasonographic variable were derived by using published data for: the difference in RI pre- and post-diuretic ($\geq +7\%$) (6), the RIR (≥ 1.10) (9), and the size of the kidneys by published age-dependent charts, with two standard deviations above the mean considered hypertrophied and two standard deviations below the mean considered small for age (17); and clinical experience and intuition for: the RIR post-diuretic (≥ 1.10) the difference in RIR pre- and post- diuretic ($\geq +7\%$), the thickness of parenchymal rims ($\leq 5\text{mm}$) and the ureteral diameter ($\geq 10\text{mm}$). Age and resistive indices pre- and post- diuretic were entered as categorical values.

The initial screening of variables was performed by using univariate analysis of association between each variable and the presence or absence of urinary tract obstruction. Values were considered significantly different when the p value was less than 0.05. These analyses were performed as an initial screening to facilitate the selection of prognosticators for the development of subsequent multivariate models, similar to the approach used by Taylor et al (18). From those results of the primary analyses, the significant variables were selected to be submitted to stepwise logistical regression models in order to identify potential predictors for urinary tract obstruction. The logistical regression model gives the probability that the outcome occurs as an exponential function of the independent variables. Mathematically, the model is expressed as: $p_x = 1 / 1 + \exp [-(b_0 + b_1x_1 + b_2x_2 + b_kx_k)]$, where k is the number of possible ultrasonographic prognosticators (x) for urinary tract obstruction ($x_1, x_2, x_3, \dots, x_k$), b_0 is the intercept, and b_1, b_2, b_k are the regression coefficients, or parameter estimates (19). The logistical

regression equation states that the predicted probability of having urinary tract obstruction is a function of the different prognosticators present, where the parameter estimate is a weighted coefficient for the different variables. A variable will be relatively influential if its parameter estimate is large and will be relatively unimportant if the parameter estimate is close to zero. Step selections are based on the maximum likelihood ratio method. Beginning with only the constant in the model, a different variable is entered into the equation in order of importance if its addition improves the existing model with a p value of 0.05 or less. Variables which do not meet the alpha entry of 0.05 are not included into the equation.

After the examination of eight basic multivariate models, the best overall model was chosen that maximized the number of predictors included as well as the sensitivity of the model. The parameter estimates of the model were then used to predict the likelihood of urinary tract obstruction in all of the subjects. The obstructive score was subsequently obtained by adjusting the parameter estimates for each variable in the logistic model found to be significant to whole numbers. The resultant obstructive score was comprised of whole number weights for each of the predictor variables which were added together. Lower scores predicted a low risk for having urinary tract obstruction and higher scores, in turn, predicted a relatively higher risk of obstruction.

DATA ANALYSIS

The data were entered into the Statistical Analysis Software© (SAS) program database and the necessary statistical calculations were performed. For the analyses of univariate variables, the differences in the proportions between the outcome groups for each categorical independent variable were analyzed with the contingency table analysis

and the Pearson Chi-square statistical test. When the statistical program revealed that 25% of the cells had expected counts less than 5, the Fisher's Exact test was utilized. For the differences in the proportions between each categorical independent variable, the odds ratios were calculated using Epi Info©, the software for epidemiological and disease surveillance. The differences in means between two groups for continuous variables were analyzed with the Student t -test. All of the univariate tests were two-tailed and significance was considered at $p \leq .05$. As described in the previous section, logistic regression was performed on all of the variables deemed significant based on the univariate analyses and the obstructive multivariable scoring system was subsequently generated.

RESULTS

Of the 320 children involved in the investigation, there were 145 female subjects and 175 male patients. Average patient age was 2.73 years with a range of 1 day to 18 years. The nonobstructed patients were older than the obstructed subjects with an average age of 35.3 months compared to 19.9 months.

Ultrasound examination revealed hydronephrosis in 376 renal units and normal collecting systems in 259 kidneys. Of those renal units seen to have hydronephrosis, 106 of them were determined to be obstructed by further radionuclide and radiographic studies. Seven patients possessed bilateral renal obstruction. Of those five patients who had a solitary kidney, four were diagnosed as having obstruction. None of the kidneys without hydronephrosis were seen to be obstructed. Etiologies for the 153 hydronephrotic, nonobstructed kidneys included vesicoureteral reflux, nonobstructed, nonrefluxing megaureter, previous posterior urethral valves, myelodysplasia, prune-belly syndrome, and nonobstructive ureteropelvic junction narrowing. Etiologies for those renal units determined as being obstructed included ureteropelvic junction obstruction, ureterovesical junction obstruction, obstructed ureteroceles, obstructed megaureters, ectopic ureteral insertions, renal calculi, and posterior urethral valves.

UNIVARIATE ANALYSIS

Table 2 lists the results of the initial univariate analyses for each of the independent variables and the presence or absence of urinary tract obstruction. Each of the variables analyzed, with the exception of the resistive index before as well as after diuretic administration, was associated with a significantly higher frequency of urinary

tract obstruction. Since the p values for many of the variables were found to be the same (0.0000), it is not possible from the univariate analyses alone to determine which variable had the strongest association with the presence of urinary tract obstruction.

TABLE 2

VARIABLES ASSOCIATED WITH INCREASED RISK OF URINARY TRACT OBSTRUCTION BY UNIVARIATE ANALYSES

Variable	p value
Resistive Index	0.1052
Resistive Index after diuretic	0.1555
Resistive Index difference with diuretic $\geq 7\%$	<0.0001
Resistive Index Ratio ≥ 1.10	<0.0001
Resistive Index Ratio after diuretic ≥ 1.10	<0.0001
Resistive Index Ratio difference with diuretic $\geq 7\%*$	0.0020
Ureteral diameter $\geq 10\text{mm}$	<0.0001
Absence of peristalsis	<0.0001
Kidney size ≥ 2 S.D. above mean for age	<0.0001
Contralateral hypertrophy	<0.0001
Increased echogenicity	<0.0001
Parenchymal rims $\leq 5\text{mm}$	<0.0001
* Determined with the Fisher's Exact test	

MULTIVARIATE ANALYSIS

Logistic regression was performed on those variables found to be significant in Table 2. Eight basic multivariate models were analyzed and because complete data was not available for all of the subjects, the two models that included all of the relevant data and maximized the sensitivity of the overall model were chosen for constructing the multivariate scoring system. The variables which contained the least amount of data were the resistive index ratio (N=147) and the difference in the resistive index after diuretic administration (N=112). The statistical program utilized could not perform logistic regression with both of these variables in the same model. Thus, two separate models which included identical variables except for the RIR and the difference in RI after diuretic administration were constructed and the parameter estimates were averaged together for the purpose of constructing the obstructive scoring system (Tables 3, 4 and 5).

TABLE 3

VARIABLES ASSOCIATED WITH URINARY TRACT OBSTRUCTION BY LOGISTIC REGRESSION IN MODEL #1

Variable	P.E.	Odds Ratio	95% CI [#]	p value ⁺⁺	S.E.
Increased echogenicity	1.5123	4.54	1.87, 11.03	0.0011	0.4533
Parenchymal rims \leq 5mm	2.2229	9.23	4.07, 20.91	0.0001	0.4171
Contralateral hypertrophy	1.2389	3.45	1.56, 7.63	0.0223	0.4044
Resistive Index ratio \geq 1.10	2.5912	13.35	4.77, 37.26	0.0001	0.5239
Ureteral diameter \geq 10mm	0.9150	2.50	1.13, 5.48	0.0234	0.4009
Absence of Peristalsis	1.5040	4.50	1.53, 13.18	0.0149	0.5483

TABLE 4

VARIABLES ASSOCIATED WITH URINARY TRACT OBSTRUCTION BY LOGISTIC REGRESSION IN MODEL #2

Variable	P.E.	Odds Ratio	95% CI [#]	p value ⁺⁺	S.E.
Increased echogenicity	1.2463	3.48	0.92, 13.18	0.0192	0.6798
Parenchymal rims \leq 5mm	1.9263	6.86	2.05, 22.90	0.0001	0.6147
Contralateral hypertrophy	1.3457	3.84	1.25, 11.75	0.0134	0.5703
Resistive Index difference with diuretic \geq 7 %	2.6377	13.98	3.38, 57.77	0.0001	0.7239
Ureteral diameter \geq 10mm	1.0268	2.79	0.74, 10.55	0.0338	0.6781
Absence of peristalsis	1.5834	4.87	1.79, 13.23	0.0001	0.5098

Note: PE= parameter estimate, CI= confidence interval, SE= standard error.

[#] 95% CI= [e^{coeff} \pm 1.96 (S.E.)]

⁺⁺ p value based on partial F at the final step of the logistic model, controlling for all other variables in the model.

TABLE 5

AVERAGE OF THE PARAMETER ESTIMATES OF THE VARIABLES ASSOCIATED WITH URINARY TRACT OBSTRUCTION

Variable	Averaged Parameter Estimates	Calculated Odds Ratio
Increased echogenicity	1.3793	3.97
Parenchymal rims $\leq 5\text{mm}$	2.0746	7.96
Contralateral hypertrophy	1.2923	3.64
Resistive Index Ratio ≥ 1.10	2.5912	13.35
Resistive Index difference with diuretic $\geq 7\%$	2.6377	13.98
Ureteral diameter $\geq 10\text{mm}$	0.9709	2.64
Absence of peristalsis	1.5437	4.68

The presence of the following sonographic variables were found to be significantly associated with a higher risk of having urinary tract obstruction: increased echogenicity, parenchymal rim thickness $\leq 5\text{mm}$, contralateral hypertrophy, ureteral diameter $\geq 10\text{mm}$, the absence of peristalsis, the resistive index ratio ≥ 1.10 , and the difference in resistive index pre- and post- diuretic $\geq 7\%$. The resistive index ratio and the difference in the resistive index after diuretic administration proved to be the strongest sonographic indicators of urinary tract obstruction, with odds ratios of 13.35 and 13.98, respectively. The diameter of the dilated ureter $\geq 10\text{ mm}$ was shown to have the least predictive ability of the significant variables, possessing an odds ratio of 2.64.

THE OBSTRUCTIVE MULTIVARIATE SCORING SYSTEM

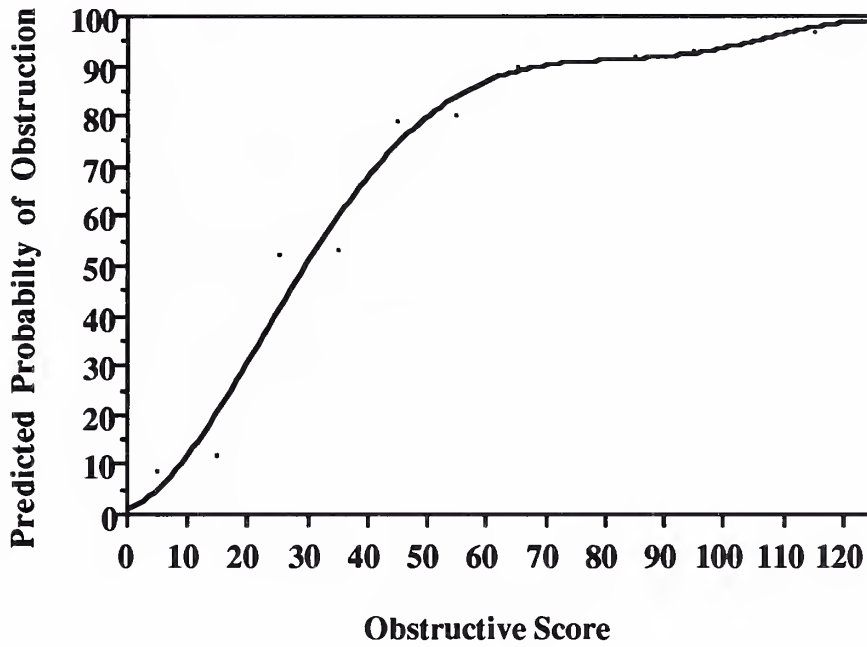
The mean parameter estimates of the variables in the logistic model were multiplied by 10 and rounded to whole numbers to produce an obstructive multivariate scoring system (Table 6). A patient's predicted probability of having urinary tract obstruction can be estimated by adding the individual numbers of those sonographic criteria that he/she possesses and reading the score from the nomogram (Figure 17). For example, if a patient is seen to have renal parenchymal rims $\leq 5\text{mm}$ (partial score= 21), increased echogenicity (partial score= 14) and a resistive index ratio ≥ 1.10 (partial score =26), he or she would have a total obstructive score of 61 and a predicted probability of having urinary tract obstruction of approximately 87%. On the other hand, if a patient is found to have a ureter diameter of $\geq 10\text{mm}$ (partial score= 10) and contralateral hypertrophy (partial score= 13) with no other sonographic findings, he or she would have an obstructive score of 23, with a predicted probability of urinary tract obstruction of less than 38%.

TABLE 6*THE OBSTRUCTIVE MULTIVARIATE SCORING SYSTEM*

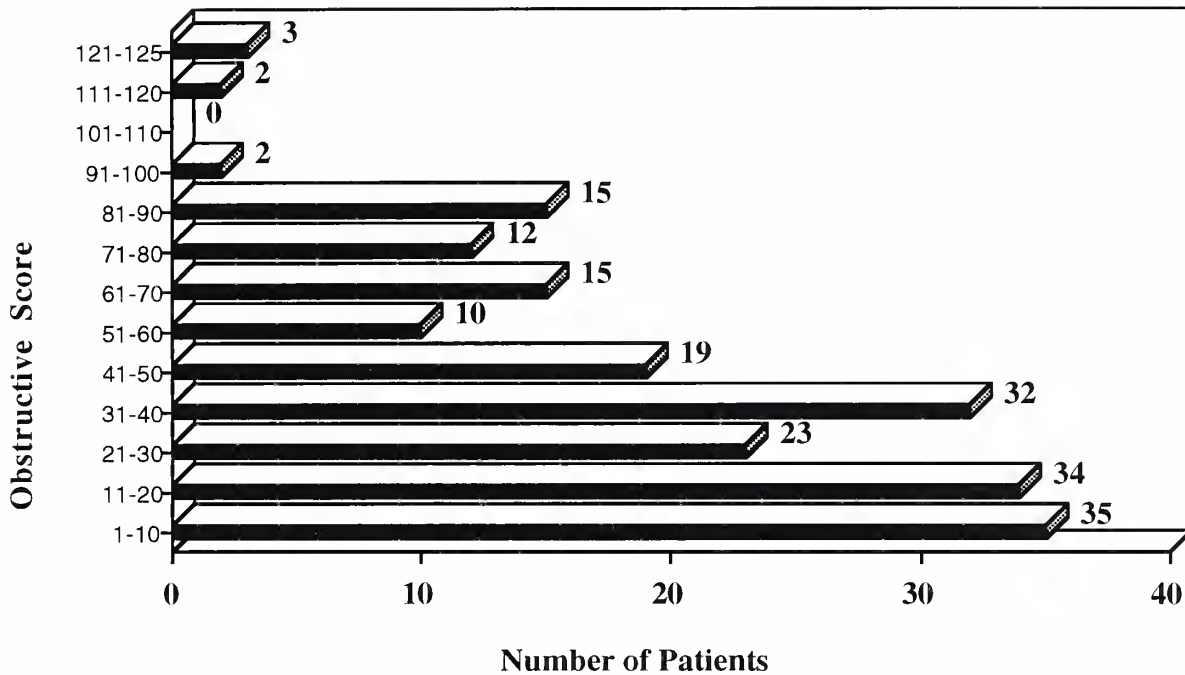
Variable	Partial Score *
Increased echogenicity	14
Parenchymal rims $\leq 5\text{mm}$	21
Contralateral hypertrophy	13
Resistive Index Ratio ≥ 1.10	26
Resistive Index difference with diuretic $\geq 7\%$	26
Ureteral diameter $\geq 10\text{mm}$	10
Absence of peristalsis	15

* The total score for a patient is derived from the summation of the partial scores for the particular sonographic variables present in each patient.

FIGURE 17. Nomogram displaying the predicted probability of urinary tract obstruction by the obstructive scoring system.



The distribution of the range of obstructive scores of those patients scoring higher than zero can be seen in Figure 18. With progressively higher scores, the number of patients found to have urinary tract obstruction increased. The subjects were further divided into three groups based on their predicted probability of having urinary tract obstruction: the low risk group (score ≤ 20 , predicted probability $\leq 30\%$), the intermediate risk group (score 21-39, predicted probability 31-67%) and the high risk group (score ≥ 40 , predicted probability $\geq 68\%$). These three groups of patients and their associated frequency of having urinary tract obstruction are shown in Table 7.

FIGURE 18**TABLE 7***URINARY TRACT OBSTRUCTION IN RISK GROUPS*

	Low ≤ 20 (N=502)	Intermediate 21-39 (N=54)	High ≥ 40 (N=79)
Obstruction	7	25	74
No Obstruction	495	29	5

Seven of the patients in the low risk group were discovered on follow-up radiographic or radionuclide examinations to possess urinary tract obstruction. Five of these patients had a mild obstruction at the level of the ureteropelvic junction which

neither demonstrated an elevated resistive index ratio nor an increase in the resistive index following the administration of furosemide. In addition, the patients showed active peristalsis in their dilated ureters. Another patient was seen to have bilateral hydronephrosis by sonography; however, while his left kidney displayed no ureteral peristalsis, increased echogenicity and a parenchymal rim of 5mm, his right kidney showed active peristalsis, normal echogenicity and a parenchymal rim of 8mm. Neither renal unit showed an increase in the resistive index following the administration of furosemide. The patient was subsequently found to have posterior urethral valves. The only abnormal study finding in the seventh patient, in addition to the hydronephrosis, was an elevated resistive index ratio. He demonstrated normal ureteral peristalsis, a ureteral diameter less than one centimeter and a parenchymal rim of 7mm. On radionuclide examination, he was found to have a ureteropelvic junction obstruction in his left kidney.

Five patients in the high-risk category were found not to have obstruction on follow-up radionuclide or radiographic examinations. Three of these patients demonstrated hydronephrosis with contralateral hypertrophy, a increased ureteral diameter and a parenchymal rim of 2 mm, 1 mm and 5 mm, respectively, giving them a total obstructive score of 44. Further radionuclide examination demonstrated no obstruction present in all three patients. Another patient was given an obstructive score of 52 since he showed no observable ureteral peristalsis, contralateral hypertrophy, a ureteral diameter of 10 mm, increased echogenicity, a resistive index ratio of 1.03 and no change in resistive index following furosemide administration. On follow-up examinations, he was discovered to have no obstructive uropathy present. The fifth patient was seen to have a dilated lower pole moiety in his left kidney. The resistive index ratio was elevated compared to both the left upper pole moiety as well as the right kidney. He had a dilated left ureter which demonstrated peristalsis and a parenchymal rim of

3mm in the lower pole of his left kidney. However, on voiding cystourethrography, he demonstrated Grade V reflux and no evidence of obstruction on intravenous pycelography.

Twenty-five patients in the intermediate group were found to have urinary tract obstruction on follow-up examinations, while 29 subjects were discovered not to have obstruction. The majority of these patients possessed only a few of the predictors of urinary tract obstruction or may have demonstrated only one of the more powerful predictors, such as an elevated resistive index ratio, a significant increase in the resistive index following diuretic administration, or a renal parenchymal rim of less than 5 mm.

A low score on the obstructive scoring scheme excludes obstruction with a specificity of 99% and a false negative rate of 9.0%. A high score on the scoring system has a sensitivity for detecting obstruction of 91% and a false positive rate of 1.0%. The intermediate scores are virtually indeterminate. The accuracy of the obstructive scoring system is 97.9%.

DISCUSSION

Unrelieved urinary tract obstruction has been shown to interfere with the normal development of the pediatric kidney. The end result is unfortunate if development of the kidney is stunted and permanent renal atrophy and destruction ensue. However, many of the etiologies of urinary tract obstruction are either surgically correctable or can be treated medically. Thus, the accurate detection of obstruction is a necessity for the pediatric patient in whom the recovery or retainment of normal renal function is the primary goal.

Diuretic renography is presently considered to be the gold standard in the evaluation of obstructive hydronephrosis in the pediatric population. However, radionuclide renography is not without its limitations, risks, and side-effects. Renography uses ionizing radiation, is expensive, invasive, and results in a 10-15% false positive rate. Sonography, on the other hand, is a less costly, noninvasive, nonionizing method used to evaluate renal morphology as well as physiology. Thus, sonography is especially ideal when the patients involved are infants and young children. However, the use of sonography in the evaluation of urinary tract obstruction has been extensively criticized, being labeled as a non-specific detector of dilatation of the renal collecting system with high false positive as well as false negative rates. These criticisms have begun to be addressed throughout the past few years with the introduction of refinements and new applications in diagnostic sonography for distinguishing obstructive from nonobstructive hydronephrosis.

Several sonographic indices have individually proven to be useful indicators for the differentiation of obstructive from nonobstructive hydronephrosis in the pediatric population. However, the utility of evaluating and comparing all of the aforementioned

sonographic parameters as well as other clinically-suspect variables to determine the strongest sonographic predictors for urinary tract obstruction had not been attempted before this clinical investigation.

This study began with the investigation of several sonographic indices in order to identify those variables which aided in the differentiation of obstructive from nonobstructive hydronephrosis. Those variables found to be significant on preliminary analyses were subsequently incorporated into a scoring system with the purpose being to sonographically identify which children are at the greatest risk of possessing urinary tract obstruction.

Our data demonstrate that the presence of the following sonographic variables are found to be significantly associated with a higher risk of having urinary tract obstruction: increased renal parenchymal echogenicity, parenchymal rim thickness $\leq 5\text{mm}$, contralateral hypertrophy, ureteral diameter $\geq 10\text{mm}$, the absence of ureteral peristalsis, the resistive index ratio ≥ 1.10 , and the difference in resistive index following diuretic administration $\geq +7\%$. The strongest predictors of obstruction were the resistive index ratio, the difference in resistive index with diuretic, and the thickness of the parenchymal rims. The weakest predictor was determined to be the diameter of the dilated ureters. All of these variables were incorporated into a scoring scheme and each renal unit was assigned a total obstructive score. According to their total score, the kidneys were divided into a low, intermediate or high risk category for possessing obstruction of the urinary tract. A low score excluded obstruction with a specificity of 99% and a false negative rate of 9.0%. The high scores had a sensitivity for detecting obstruction of 91% and a false positive rate of 1.0%. The renal units in the intermediate category had an approximately equal chance of either being obstructed (25/54) or nonobstructed (29/54),

which converts the intermediate category into an indeterminate one and makes the differentiation of obstruction from nonobstruction impossible in this category.

Not surprisingly, the obstructive scoring system is not 100% sensitive or specific. Because the scoring system focuses solely on certain specific sonographic findings, one must keep in mind that many other important factors such as clinical suspicion, the sonographic appearance of the kidney as a whole, and renal function must also be considered when sonographers attempt to distinguish obstructive from nonobstructive hydronephrosis. However, when the scoring scheme is used as a general guideline, it does indeed provide a basic framework through which sonographers can evaluate and identify those children with urinary tract obstruction.

A strength of this study is that it is the first to examine several sonographic variables of the pediatric urinary tract simultaneously and to construct a scoring scheme using these variables for the differentiation of obstructive from nonobstructive hydronephrosis in children. However, limitations of this study need to be addressed. Due to the nature of a retrospective study, all of the patients did not undergo all radiographic and radionuclide examinations. Thus, the obstructive scoring system needed to be constructed as an average of two logistic regression models. Although the parameter estimates were, for the most part, quite numerically similar, the averaging of the two numbers might have biased the scoring scheme in some unknown manner. However, the majority of the patients seemed to be placed in the correct risk category for possessing urinary tract obstruction based on their multivariate score with only 7 of the 502 kidneys in the low-risk category having urinary tract obstruction and 5 of the 79 renal units in the high-risk category not possessing obstruction. Thus, despite its limitations, the scoring system appears to work in clinical practice.

Another limitation seen in clinical practice is the often ignored dynamic nature of urinary tract obstructions, particularly those at the ureteropelvic junction. At times, these systems may be nonobstructed; yet, with an increase in urine flow rates and a change in the geometry at the ureteropelvic junction, intermittent acute obstructive uropathy may painfully precipitate (Dietl's crisis). However, if the kidney is imaged between crises, it may test normal, or nearly normal, and nonobstructed.

In the future, if the obstructive scoring system becomes widely accepted, those children in the high-risk category for possessing urinary tract obstruction can be spared further expensive, time-consuming, ionizing and invasive examinations to corroborate the diagnosis of obstruction. The patients assigned to the low-risk category also can obviate the need for any additional radiographic and radionuclide examinations and subsequently, the hydronephrosis may be followed with serial sonographic examinations. However, if vesicoureteral reflux is suspected, it may be prudent for these patients to undergo a voiding cystourethrogram to establish the diagnosis. Due to the indeterminate results of the intermediate-risk category, children assigned to this group will need to undergo further radionuclide examinations, such as the diuretic radionuclide renogram, to more accurately evaluate the etiology of the hydronephrosis. However, if those patients assigned to the low or intermediate risk categories develop any additional sonographic or clinical indications suggesting urinary tract obstruction, further testing is of the utmost necessity for the differentiation of their hydronephrosis.

In summary, the data demonstrates that the obstructive scoring system excludes urinary tract obstruction in children in the low risk category with a specificity of 99% and detects obstruction in the high risk category with a sensitivity of 91%. This study lays the foundation for further prospective clinical investigation into the utility and reliability of

the obstructive multivariate scoring system, and the evaluation and refinement of these criteria by other investigators would be welcomed.

CONCLUSION

Several ultrasonographic variables appear to be effective predictors for the differentiation of obstructive from nonobstructive hydronephrosis in children. The application of these variables in the obstructive scoring system shows great promise for sonographically predicting which children possess urinary tract obstruction and which do not, and one day, may obviate the need for more invasive and ionizing radiographic and radionuclide examinations in the pediatric population.

REFERENCES

INTRODUCTION

PART I

ANATOMY OF THE URINARY SYSTEM

1. Moore, K.L. *Clinically oriented anatomy*, Williams and Wilkins, 1985, 252-268
2. Amis, E. S. and Newhouse, J.H. *Essentials of uroradiology*, Little, Brown and Company, 1991, 6-11.
3. Moell, H. Size of normal kidneys. *Acta Radiologica* 1956; 46:640.
4. Schneck, C.D. Sectional anatomy of the genitourinary system.. In Resnick, M.I. and Rifkin, M.D. *Ultrasonography of the Urinary Tract*, Williams and Wilkins, 1991, 34-58.
5. Hanna, M.K. et al. Ureteral structure and ultrastructure. Part I: The normal human ureter. *Journal of Urology* 1976, 116: 718.
6. Amis, E.S. and Newhouse, J.H. *Essentials of uroradiology*, Little, Brown and Company, 1991, 11-13.
7. Moore, K.L. *Clinically oriented anatomy*, Williams and Wilkins, 1985, 359-365.

EMBRYOLOGY OF THE URINARY SYSTEM

1. Amis, E.S. and Newhouse, J.H. *Essentials of uroradiology*, Little, Brown and Company, 1991, 3-4.
2. Moore, K.L. *The developing human: clinically oriented embryology*, W.B. Saunders Company, 1988; 246-256.
3. Fitzgerald, M.J. *Human embryology: a regional approach*, Harper and Row, 1978.
4. Moore, K.L. *The developing human: clinically oriented embryology*, W.B. Saunders Company, 1988, 257-259.

PHYSIOLOGY OF THE URINARY SYSTEM

1. Lecture, F.S. Wright, Physiology, Yale University School of Medicine, 1992.
2. Guyton, A.C. *Textbook of medical physiology*. W.B. Saunders company, 1991, 273-353.
3. Amis, E.S. and Newhouse, J.H. *Essentials of uro radiology*, Little, Brown and Company, 1991, 16-17.
4. Ganong, W.F. *Review of medical physiology*. Appleton and Lange, 1991, 649-679.
5. Hanna, M.K. et al. Ureteral structure and ultrastructure. Part I: The normal human ureter. *Journal of Urology* 1976, 116: 718.

PART II

URINARY TRACT OBSTRUCTION

1. Rao, B.K. and Bryan, P.J. Sonography of acute and chronic renal failure. In Resnick, M.I. and Rifkin, M.D. (Eds.) *Ultrasonography of the urinary tract*, Williams and Wilkins, 1991, 223.
2. Amis, E.S. and Newhouse, J.H. *Essentials of uro radiology*, Little, Brown and Company, 1991, 233-234.
3. Robbins, S.L., Contran, R.S. and Kumar, V. *Pathologic basis of disease*, W.B. Saunders Company, 1989, 1071-1073.
4. Klahr, S., et al. Urinary tract obstruction. In Brenner, B.M. and Rector, F. (eds.): *The Kidney*. 3rd ed. Philadelphia, W.B. Saunders Company, 1986, 1443-1490.
5. Robbins, S.L., Contran, R.S. and Kumar, V. *Pathologic basis of disease*, W.B. Saunders Company, 1989, 1084-1085.
6. Elkin, M. Radiological observations in acute renal obstruction. *Radiology* 1963, 81: 484.
7. Elkin, M. Obstructive uropathy and uremia. *Radiology Clinics of North America* 1972, 10: 421.
8. Djurhaus, J.C. et al. Experimental hydronephrosis. *Acta Chirurgia Scandinavica* 1976, 472: 345.
9. Joeke, A.M. Obstructive uropathy. *Seminars in Nuclear Medicine* 1974, 4:187.

10. Arruda, J.A.L. Obstructive uropathy, *Contemporary issues in nephrology* 1983, 10: 248.

ETIOLOGIES OF URINARY TRACT OBSTRUCTION IN THE PEDIATRIC POPULATION

1. Macfarlane, M.T. *Urology for the house officer*, Williams and Wilkins, 1988, 73-77.
2. Sumner, T.E. Ultrasound in pediatric urology. In Resnick, M.L. and Rifkin, M.D. (Eds), *Ultrasonography of the Urinary Tract*, Williams and Wilkins, 1991, 377.
3. Sumner, T.E. Ultrasound in pediatric urology. In Resnick, M.L. and Rifkin, M.D. (Eds.) *Ultrasonography of the Urinary Tract*, Williams and Wilkins, 1991, 366.
4. Sumner, T.E. Ultrasound in pediatric urology. In Resnick, M.L. and Rifkin, M.D. (Eds.) *Ultrasonography of the Urinary Tract*, Williams and Wilkins, 1991, 366-369.
5. Amis, E.S. and Newhouse, J.H. *Essentials of uroradiology*, Little, Brown and Company, 1991, 260-262.
6. Sumner, T.E. Ultrasound in pediatric urology. In Resnick, M.L. and Rifkin, M.D. (Eds.) *Ultrasonography of the urinary tract*, Williams and Wilkins, 1991, 369-374.
7. Sumner, T.E. Ultrasound in pediatric urology. In Resnick, M.L. and Rifkin, M.D. (Eds.) *Ultrasonography of the urinary tract*, Williams and Wilkins, 1991, 374-377.

OTHER CAUSES OF HYDRONEPHROSIS

1. Aaronson, I.A. and Cremin, B.J. *Clinical paediatric uroradiology*, Churchill Livingstone, 1984, 431.
2. Levitt, S.B. and Weiss, R.A. Vesicoureteral reflux. In Kelalis, P.P., King, L.R. and Belman, A.B. (eds.): *Clinical Pediatric Urology*, W.B. Saunders Company, 1985, 355-380.
3. Brant, W.E. and Helms, C.A. *Fundamentals in diagnostic radiology*, Williams and Wilkins, 1994, 784-786.
4. Aaronson, I.A. and Cremin, B.J. *Clinical paediatric uroradiology*, Churchill Livingstone, 1984, 123-129.

5. King, L.R. Ureter and ureterovesical junction. In Kelalis, P.P., King, L.R. and Belman, A.B. (Eds.): *Clinical Pediatric Urology*, W.B. Saunders Company, 1985, 497-498.
6. Rink, R.C., Adams, M.C., and Mitchell, M.E. Ureteral abnormalities. In Ashcraft, K.W. (Ed.) *Pediatric Urology*, W.B. Saunders Company, 1990, 144-146.
7. Amis, E.S. and Newhouse, J.H. *Essentials of uroradiology*, Little, Brown and Company, 1991, 62.
8. Ashcraft, K.W. Prune belly syndrome. In Ashcraft, K.W. (Ed.) *Pediatric Urology*, W.B. Saunders Company, 1990, 257-267.
9. Aaronson, I.A. and Cremin, B.J. *Clinical paediatric uroradiology*, Churchill Livingstone, 1984, 255-265.
10. Rao, B.K. and Bryan, P.J. Sonography of acute and chronic renal failure. In Resnick, M.L. and Rifkin, M.D. *Ultrasonography of the urinary tract*, Williams and Wilkins, 1991, 224.

PART III

HISTORY OF DIAGNOSTIC ULTRASOUND

1. Curie, I. and Curie, P. Development par pression de l'electricite polaire dans les cristaux hemiedres a faces inclinees. *Compt Rend 1880*; 91: 294.
2. Brown, R.E. *Ultrasonography: basic principles and clinical applications*, Warren H. Green, Inc., 1975 , 3.
3. Brown, R.E. *Ultrasonography: basic principles and clinical applications*, Warren H. Green, Inc., 1975, 23-28.
4. Solokov, S.Y. Ultra-acoustic methods of finding internal defects in metal objects, *Zavodskaya Laboratoruza 1935*; 4:1468.
5. Solokov, S.Y. Means for indicating flaws in materials, *U.S. Patent 2* , 16, 125, 1939.
6. Firestone, F. The supersonic reflectoscope, and instrument for inspecting the interior of solid parts by means of sound waves, *J Acoust Soc Amer 1946*; 17:287.
7. Ballantine, H.T., Bolt, R.H., Heutner, T.F. , et al. On the detection of intracranial pathology by ultrasound, *Science 1950*; 112:525.
8. Guttner, W., Fielder, G., Patzold, J. Uber ultraschallabbidungem am menschlichen schadel, *Acoustica 1952*; 2:148.

9. Ludwig, G.D. and Struthers, F.W. Consideration underlying the use of ultrasound to detect gallstones and foreign bodies in tissue, *Naval Medical Research Institute* 1949; 4:1-23.
10. Wild, J. The use of ultrasonic pulses for the measurement of biologic tissues and the detection of tissue density changes, *Surgery* 1950; 27:183-188.
11. French, L., Wild, J., and Neal, D. Detection of cerebral tumors by ultrasonic pulses. *Cancer* 1950; 3:705.
12. Wild, J. and Reid, J. Further pilot echographic studies on the histologic structure of tumors of the living intact human breast. *American Journal of Pathology* 1952;28:839-861.
13. Wild, J. and Reid, J. Echographic tissue diagnosis, In *Proceedings of the Fourth Annual Conference on Ultrasonic Therapy*, Detroit, 1955, 1.
14. Howry, D.H. Techniques used in ultrasonic visualization of soft tissues, In Kelly, E. (Ed.) *Ultrasound in Biology and Medicine*, American Institute of Biological Sciences, 1957, 49.
15. Holmes, J., Wright, W., Meyer, E., et al. Ultrasonic contact scanner for diagnostic application, *American Journal of Medical Electronics* 1965; 4:147.
16. White, D.N. The conception, birth and childhood of WFUMB and its specialist and continental federations: the first quarter century, *Ultrasound in Medicine and Biology* 1990, 16: 333-348.
17. White, D.N., Clark, G., Carson, J., White, E. (Eds). *Ultrasound in biomedicine, introduction*, Pergamon Press, 1982, 120-125.
18. Beach, K.W. 1975-2000: a quarter century of ultrasound technology, *Ultrasound in Medicine and Biology* 1992, 18: 377-388.
19. Elkin, M. Stages in the growth of uro-radiology, *Radiology* 1990, 175: 297-306.
20. Tablin, G.V., Meridith, O.M., Kade, H, and Winters, C.C. The radioisotope renogram: an external test for individual kidney function and upper urinary tract patency, *Journal of Laboratory Clinical Medicine* 1956, 48: 886-901.

PHYSICS OF DIAGNOSTIC ULTRASOUND

1. Brant, W.E. Diagnostic imaging methods. In Brant, W.E. and Helms, C.A. (Eds.) *Fundamentals in diagnostic radiology*, Williams and Wilkins, 1994, 13-14.

2. Burns, P.N. Ultrasound imaging and doppler: principles and instrumentation. In Resnick, M.L. and Rifkin, M.D.(Eds). *Ultrasonography of the urinary tract*, Williams and Wilkins, 1991, 1-33.
3. Brown, R.E. *Ultrasonography: basic principles and clinical applications*, Warren H. Green, Inc., 1975 , 3-28.
4. Kremkau, F.W. *Diagnostic Ultrasound: Principles, instruments and exercises*. W.B. Saunders, 1989, 4-16.

DOPPLER ULTRASOUND

1. Brown, R.E. *Ultrasonography: basic principles and clinical applications*, Warren H. Green, Inc., 1975, 20-22.
2. Brant, W.E. and Helms, C.A. *Fundamentals in diagnostic radiology*, Williams and Wilkins, 1994, 15-16.
3. Wells, P.N.T. Basic principles and doppler physics. In Taylor, K.J.W., Burns, P.N. and Wells, P.N.T. (Eds). *Clinical Applications of Doppler Ultrasound*, Raven Press, 1988, 1-25.
4. Burns, P.N. Ultrasound imaging and doppler: principles and instrumentation. In Resnick, M.L. and Rifkin, M.D.(Eds). *Ultrasonography of the urinary tract*, Williams and Wilkins, 1991, 20-33.
5. Kremkau, F.W. *Doppler ultrasound: principles and instruments*, W.B. Saunders Company, 1990, 101-104.
6. Burns, P.N. Interpretation of doppler signals. In Taylor, K.J.W., Burns, P.N. and Wells, P.N.T. (Eds). *Clinical Applications of Doppler Ultrasound*, Raven Press, 1988, 102-116.

PART IV

PRENATAL SCREENING OF HYDRONEPHROSIS

1. Wheeler, T. and Jeanty, P. The dilated fetal renal tract: imaging and prenatal management. In Nielson, J.P. and Chambers, S.E. *Obstetric Ultrasound 1*, Oxford University Press, 1993, 102-115.

2. Chudleigh, P. and Pearce, J.M. *Obstetric Ultrasound: how, why, and when*, Churchill Livingstone, 1992, 112-114.
3. Shkolnik, A. Ultrasonography of the urogenital system. In Kelalis, P.P., King, L.R. and Belman, A.B. (eds.): *Clinical Pediatric Urology*, W.B. Saunders Company, 1985, 183-186.
4. Arger, P.H., Coleman, B.G., Mintz, M.C., et al. Routine fetal genitourinary tract screening, *Radiology* 1985, 156, 485-489.
5. Hobbins, J.C., Romero, R., Grannum, P., Berkowitz, R., Cullen, M., and Mahoney, M. Antenatal diagnosis of renal anomalies with ultrasound. *American Journal of Obstetrics and Gynecology* 1984, 148, 868-875.
6. Golbus, M.S., Filly, R.A., Callan, P.W., Glick, P.L., Harrison, M.R. and Anderson, R.L. Fetal urinary tract obstruction: management and selection for treatment, *Seminars in Perinatology* 1985, 9:91.

DIAGNOSIS OF URINARY TRACT OBSTRUCTION IN THE PEDIATRIC POPULATION

1. Najmaldin, A.S., Burge, D.M., and Atwell, J.D. Outcome of antenatally diagnosed pelviureteric junction hydronephrosis, *British Journal of Urology* 1991, 67:96-99.
2. Laing, F., Burke, V., and Wing, V. Postpartum evaluation of fetal hydronephrosis: optimal timing for followup sonography. *Radiology* 1984, 152:423.
3. Majd, M. Nuclear medicine. In Kelalis, P.P., King, L.R. and Belman, A.B. (eds.): *Clinical Pediatric Urology*, W.B. Saunders Company, 1985, 149-156.
4. Slovis, T.L., Sty, J.R., and Haller, J.O. *Imaging of the pediatric urinary tract*. W.B. Saunders Company, 1989, 8-9.
5. Morrison, S.C. and Caldamone, A.A. Imaging. In Ashcraft, K.W. (Ed.) *Pediatric Urology*, W.B. Saunders Company, 1990, 13-15.
6. Aaronson, I.A. and Cremin, B.J. *Clinical paediatric uroradiology*, Churchill Livingstone, 1984, 132-136.
7. Slovis, T.L., Sty, J.R., and Haller, J.O. *Imaging of the pediatric urinary tract*. W.B. Saunders Company, 1989, 10-12.
8. Aaronson, I.A. and Cremin, B.J. *Clinical paediatric uroradiology*, Churchill Livingstone, 1984, 136-137.
9. Aaronson, I.A. and Cremin, B.J. *Clinical paediatric uroradiology*, Churchill Livingstone, 1984, 17-23.

10. Slovis, T.L., Sty, J.R., and Haller, J.O. *Imaging of the pediatric urinary tract*. W.B. Saunders Company, 1989, 18-21.
11. Imray, T.J., Terry, D.W., and Dodds, W.J. The caudad angle view: a helpful adjunct in excretory urography. *Radiology* 1977, 122:253-255.
12. Brant, W.E. Diagnostic imaging methods. In Brant, W.E. and Helms, C.A. (Eds.) *Fundamentals in diagnostic radiology*, Williams and Wilkins, 1994, 3-19.
13. Whitfield, H.N., Britton, K.E., Fry, I.K. et al. The obstructed kidney: correlation between renal function and urodynamic assessment, *British Journal of Urology* 1977, 49:615.
14. Aaronson, I.A. and Cremin, B.J. *Clinical paediatric urology*, Churchill Livingstone, 1984, 26.
15. Hoffman, A. Uroradiology: procedures and anatomy. In Kelalis, P.P., King, L.R. and Belman, A.B. (eds.): *Clinical Pediatric Urology*, W.B. Saunders Company, 1985, 130-131.
16. Whitaker, R. Methods of assessing obstruction in dilated ureter, *British Journal of Urology* 1973, 45:15.
17. Morrison, S.C. and Caldamone, A.A. Imaging. In Ashcraft, K.W. (Ed.) *Pediatric Urology*, W.B. Saunders Company, 1990, 20.
18. O'Reilly, P.H., Shields, R.A., and Testa, H.J. Renography. In O'Reilly, P.H., Shields, R.A., and Testa, H.J. (Eds.) *Nuclear Medicine in Urology and Nephrology*, Butterworth and Company, 1986, 17-21.
19. Majd, M. Nuclear medicine. In Kelalis, P.P., King, L.R. and Belman, A.B. (eds.): *Clinical Pediatric Urology*, W.B. Saunders Company, 1985, 150-156.
20. Arnold, R.W. , Subramanian, G., McAfee, J.G., et al. Comparison of Tc99m complexes for renal imaging, *Journal of Nuclear Medicine* 1975, 16:357.
21. O'Reilly, P.H., Shields, R.A., and Testa, H.J. Renography. In O'Reilly, P.H., Shields, R.A., and Testa, H.J. (Eds.) *Nuclear Medicine in Urology and Nephrology*, Butterworth and Company, 1986, 9-17.
22. O'Reilly, P.H. and Lupton, E.W. Obstructive uropathy. In O'Reilly, P.H., Shields, R.A., and Testa, H.J. (Eds.) *Nuclear Medicine in Urology and Nephrology*, Butterworth and Company, 1986, 91-108.
23. Thrall, J., Koff, S., and Keyes, J. Diuretic radionuclide renography and scintigraphy in the differential diagnosis of hydroureteronephrosis, *Seminars in Nuclear Medicine* 1981, 11:89.
24. Morrison, S.C. and Caldamone, A.A. Imaging. In Ashcraft, K.W. (Ed.) *Pediatric Urology*, W.B. Saunders Company, 1990, 8-9.

25. Bude, R.O., DiPietro, M.A., Platt, J.F., and Rubin, J.M. Effect of furosemide and intravenous normal saline fluid load upon the renal resistive index in nonobstructed kidneys in children, *The Journal of Urology* 1994, 151:438-441.

DIAGNOSIS OF URINARY TRACT OBSTRUCTION BY SONOGRAPHY IN THE PEDIATRIC PATIENT

1. Slovis, T.L., Sty, J.R., and Haller, J.O. *Imaging of the pediatric urinary tract*. W.B. Saunders Company, 1989, 24-30.
2. Keller, M.S. Renal doppler sonography in infants and children, *Radiology* 1989, 172:603-604.
3. Sumner, T.E. Ultrasound in pediatric urology. In Resnick, M.L. and Rifkin, M.D. (Eds.) *Ultrasonography of the urinary tract*, Williams and Wilkins, 1991, 349.
4. Burns, P. N. Ultrasound imaging and doppler: principles and instrumentation. In Resnick, M.L. and Rifkin, M.D. (Eds.) *Ultrasonography of the urinary tract*, Williams and Wilkins, 1991, 5.
5. Aaronson, I.A. and Cremin, B.J. *Clinical paediatric urology*, Churchill Livingstone, 1984, 28-31.
6. McInnis, A.N., Felman, A.H., Kaude, J.V., and Walker, R.D. Renal ultrasound in the neonatal period, *Pediatric Radiology* 1982, 12:15-20.
7. Haller, J.O., Berdon, W.E., and Friedman, A.P. Increased renal cortical echogenicity: a normal finding in neonates and infants, *Radiology* 1978, 129:143-151.
8. Sumner, T.E. Ultrasound in pediatric urology. In Resnick, M.L. and Rifkin, M.D. (Eds.) *Ultrasonography of the urinary tract*, Williams and Wilkins, 1991, 349-351.
9. Koenigsberg, M. and Hoffman-Tretin, J. *Abdominal sonography*, J.B. Lippincott Company, 1991, 8.2-8.7.
10. Shkolnik, A. Ultrasonography of the urogenital system. In Kelalis, P.P., King, L.R. and Belman, A.B. (eds.): *Clinical Pediatric Urology*, W.B. Saunders Company, 1985, 210-211.
11. Bodner, D.R. and Resnick, M.I. Ultrasonography of the urinary bladder. In Resnick, M.L. and Rifkin, M.D. (Eds.) *Ultrasonography of the urinary tract*, Williams and Wilkins, 1991, 255-256.

12. Rao, B.K. and Bryan, P.J. Sonography of acute and chronic renal failure. In Resnick, M.L. and Rifkin, M.D. *Ultrasonography of the urinary tract*, Williams and Wilkins, 1991, 223-225.
13. Aaronson, I.A. and Cremin, B.J. *Clinical paediatric uro radiology*, Churchill Livingstone, 1984, 178-180.
14. Crombleholme, T.M., Harrison, M.R., Golbus, M.S., et al. Fetal intervention in obstructive uropathy: prognostic indicators and efficacy of intervention, *American Journal of Obstetrics and Gynecology* 1990, 162:1239-1244.
15. Aaronson, I.A. and Cremin, B.J. *Clinical paediatric uro radiology*, Churchill Livingstone, 1984, 173-174.
16. Amis, E.S. and Newhouse, J.H. *Essentials of uro radiology*, Little, Brown and Company, 1991, 58.
17. Aaronson, I.A. and Cremin, B.J. *Clinical paediatric uro radiology*, Churchill Livingstone, 1984, 44.
18. Koenigsberg, M. and Hoffman-Tretin, J. *Abdominal sonography*, J.B. Lippincott Company, 1991, 8.13-8.18.
19. Weiss, R.M. Obstructive uropathy: pathophysiology and diagnosis. In Kelalis, P.P., King, L.R. and Belman, A.B. (eds.): *Clinical Pediatric Urology*, W.B. Saunders Company, 1985, 420-425.
20. Keller, M.S., Weiss, R.M. and Rosenfield, N.S. Sonographic evaluation of ureterectasis in children: the significance of peristalsis, *The Journal of Urology* 1993, 149:553-555.
21. Weiss, R.M. and Biancani, P. Characteristics of normal and refluxing ureterovesical junctions, *Journal of Urology* 1983, 129:858.
22. Grana, I., Kidd, J., Idriss, F., and Swenson, O. Effect of chronic urinary tract infection on ureteral peristalsis, *Journal of Urology* 1965, 94:652.
23. Benzi, G., Arrigoni, E., Panceri, P., Panzarasa, R., Berte, F., and Crema, A. Effect of antibiotics on the ureter motor activity, *Japanese Journal of Pharmacology* 1973, 23:599.
24. Webb, J. A.W. Ultrasonography in the diagnosis of renal obstruction: sensitive but not very specific, *British Medical Journal* 1990, 301:944-946.
25. Rao, B.K. and Bryan, P.J. Sonography of acute and chronic renal failure. In Resnick, M.L. and Rifkin, M.D. *Ultrasonography of the urinary tract*, Williams and Wilkins, 1991, 224-228.
26. Cronan, J.J. Contemporary concepts for imaging urinary tract obstruction, *Urologic Radiology* 1992, 14:8-12.

27. Arima, M., Ishibashi, M., Usami, M. et al. Analysis of the arterial blood flow patterns of normal and allografted kidneys by the directional ultrasonic doppler technique, *The Journal of Urology* 1979, 122:587.
28. Gilbert, R., Garra, B. and Gibbons, M.D. Renal duplex doppler ultrasound: an adjunct in the evaluation of hydronephrosis in the child, *The Journal of Urology* 1993, 150:1192-1194.
29. Palmer, J.M., Lindfors, K.K., Ordorica, R.C., and Marder, D.M. Diuretic doppler sonography in postnatal hydronephrosis, *The Journal of Urology* 1991, 146:605-608.
30. Berland, L.L., Lawson, T.L., Adams, M.B., Melrose, B.L. and Foley, W.D. Evaluation of renal transplants with pulsed doppler duplex sonography, *Journal of Ultrasound in Medicine* 1982, 1:215. Rifkin, 1987
32. Vaughan, E.D., Sorenson, E.J., and Gillenwater, J.Y. The renal hemodynamic response to chronic unilateral complete ureteral occlusion, *Investigative Urology* 1970, 8:78.
33. Ryan, P.C., Maher, K.P., Murphy, B., Jurley, G.D., and Fitzpatrick, J.M. Experimental partial ureteric obstruction: pathophysiologic changes in upper tract pressures and renal blood flow, *The Journal of Urology* 1987, 138:674.
34. Platt, J.F., Rubin, J.M., Ellis, J.H. and DiPietro, M.A. Duplex doppler ultrasound of the kidney: differentiation of obstructive from nonobstructive dilatation, *Radiology* 1989, 171:709.
35. Gotlieb, R.H., Luhmann, K., IV and Oates, R.P. Duplex ultrasound evaluation of normal native kidneys and native kidneys with urinary tract obstruction, *Journal of Ultrasound in Medicine* 1989, 8:609.
36. Platt, J.F., Rubin, J.M., and Ellis, J.H. Distinction between obstructive and nonobstructive pyelocaliectasis with duplex doppler sonography, *American Journal of Radiology* 1989, 153:997.
37. Chen, J.H., Pu, Y.S., Liu, S.P. and Chiu, T.Y. Renal hemodynamics in patients with obstructive uropathy evaluated by duplex doppler sonography, *The Journal of Urology* 1993, 150:18-21.
38. Rogers, P.M., Bates, J.A., and Irving, H.C. Intrarenal doppler ultrasound studies in normal and acutely obstructed kidneys, *The British Journal of Radiology* 1992, 65: 207-212.
39. Dodd, G.D., Kaufman, P.N., and Bracken, R.B. Renal arterial duplex doppler ultrasound in dogs with urinary obstruction, *The Journal of Urology* 1991, 145:644-646.

40. Ordica, R.C., Lindfors, K.K. and Palmer, J.M. Diuretic doppler sonography following successful repair of renal obstruction in children, *The Journal of Urology* 1993, 150:774-777.
41. Kessler, R.M., Quevedo, H., Lankau, C.A. et al. Obstructive vs. nonobstructive dilatation of the renal collecting system in children: distinction with duplex sonography, *American Journal of Radiology* 1993, 160:353-357.
42. Wong, S.N., Lo, R.N.S. and Yu, E.C.L. Renal blood flow pattern by noninvasive doppler ultrasound in normal children and acute renal failure patients. *The Journal of Ultrasound in Medicine* 1989, 8:135.
43. Keller, M.S., Garcia, C.J., Korsvik, H., Weiss, R.M., Taylor, K.J.W., and Ehrenkranz, R.E. Duplex sonographic examination of children with renal collecting system dilatation. Abstract from *Society of Pediatric Radiology, April 19-22, 1990*, p.18.
44. Bude, R.O., DiPietro, M.A., Platt, J.F. , Rubin, J.M. et al. Age dependency of the renal resistive index in healthy children, *Radiology* 1992, 184:469.
45. Gilbert, R., Garra, B. and Gibbons, M.D. Renal duplex doppler ultrasound: an adjunct in the evaluation of hydronephrosis in the child, *The Journal of Urology* 1993, 150:1192-1194..
46. Keller, M.S., Garcia, C.J., Korsvik, H.E., Weiss, R.M. and Rosenfield, N.S. Resistive index ratios in the US differentiation of unilateral obstructive vs. non-obstructive hydronephrosis in children. *Pediatric Radiology* 1991, 21:462, abstract 1.
47. Palmer, J.M., Lindfors, K.K., Ordica, R.C. and Marder, D.M. Diuretic doppler sonography in postnatal hydronephrosis; *Journal of Urology, Part 2*, 1991, 146:605.
48. Keller, M.S., Korsvik, H.E., and Weiss, R.M. Diuretic doppler sonography with correlative scintigraphy in children with hydronephrosis. Abstract from the *Society of Pediatric Radiology*, 1992, May 14-17, 49.
49. Renowden, S.A. and Cochlin, D.L. The effect of intravenous furosemide on the doppler waveform in normal kidneys, *Journal of Ultrasound in Medicine* 1992, 11:65.
50. Patriquin, H., Lambert, R., Williot, P., Filiatrault, D. and Grignon, A. Doppler sonography in unilateral hydronephrosis: is the distinction between dilatation and obstruction possible? *Journal of Pediatric Radiology* 1994, abstract #1, 364.
51. Bude, R.O., DiPietro, M.A., Platt, J.F., and Rubin, J.M. Effect of furosemide and intravenous normal saline fluid load upon the renal resistive index in nonobstructed kidneys in children, *The Journal of Urology* 1994, 151:438-441.

MATERIALS AND METHODS

1. Wong, S.N., Lo, R.N.S. and Yu, E.C.L. Renal blood flow pattern by noninvasive doppler ultrasound in normal children and acute renal failure patients. *The J Journal of Ultrasound in Medicine* 1989, 8:135.
2. Keller, M.S., Garcia, C.J., Korsvik, H., Weiss, R.M., Taylor, K.J.W., and Ehrenkranz, R.E. Duplex sonographic examination of children with renal collecting system dilatation. *Abstract from Society of Pediatric Radiology, April 19-22, 1990*, p.18.
3. Bude, R.O., DiPietro, M.A., Platt, J.F. , Rubin, J.M. et al. Age dependency of the renal resistive index in healthy children, *Radiology* 1992, 184:469.
4. Gilbert, R., Garra, B. and Gibbons, M.D. Renal duplex doppler ultrasound: an adjunct in the evaluation of hydronephrosis in the child, *The Journal of Urology* 1993, 150:1192-1194.
5. Palmer, J.M., Lindfors, K.K., Ordorica, R.C. and Marder, D.M. Diuretic doppler sonography in postnatal hydronephrosis; *Journal of Urology, Part 2, 1991* , 146:605.
6. Keller, M.S., Korsvik, H.E., and Weiss, R.M. Diuretic doppler sonography with correlative scintigraphy in children with hydronephrosis. Abstract from the *Society of Pediatric Radiology, 1992, May 14-17*, 49.
7. Patriquin, H., Lambert, R., Williot, P., Filiatrault, D. and Grignon, A. Doppler sonography in unilateral hydronephrosis: is the distinction between dilatation and obstruction possible? *Journal of Pediatric Radiology* 1994, abstract #1, 364.
8. Bude, R.O., DiPietro, M.A., Platt, J.F., and Rubin, J.M. Effect of furosemide and intravenous normal saline fluid load upon the renal resistive index in nonobstructed kidneys in children, *The Journal of Urology* 1994, 151:438-441.
9. Keller, M.S., Garcia, C.J., Korsvik, H.E., Weiss, R.M. and Rosenfield, N.S. Resistive index ratios in the us differentiation of unilateral obstructive vs. non-obstructive hydronephrosis in children. *Pediatric Radiology* 1991, 21:462, abstract 1.
10. Keller, M.S., Weiss, R.M. and Rosenfield, N.S. Sonographic evaluation of ureterectasis in children: the significance of peristalsis, *The Journal of Urology* 1993, 149:553-555.
11. Weiss, R.M. Obstructive uropathy: pathophysiology and diagnosis. In Kelalis, P.P., King, L.R. and Belman, A.B. (eds.): *Clinical Pediatric Urology*, W.B. Saunders Company, 1985, 420-425.

12. Aaronson, I.A. and Cremin, B.J. *Clinical paediatric uro radiology*, Churchill Livingstone, 1984, 173-174.
13. Amis, E.S. and Newhouse, J.H. *Essentials of uro radiology*, Little, Brown and Company, 1991, 58.
14. Crombleholme, T.M., Harrison, M.R., Golbus, M.S., et al. Fetal intervention in obstructive uropathy: prognostic indicators and efficacy of intervention, *American Journal of Obstetrics and Gynecology* 1990, 162:1239-1244.
15. Aaronson, I.A. and Cremin, B.J. *Clinical paediatric uro radiology*, Churchill Livingstone, 1984, 178-180.
16. Majd, M. Avoiding pitfalls in pediatric uro radiology: diuretic renography; *Dialogues in Pediatric Urology* 1989, 12:6.
17. Han, B.K. and Babcock, D.S. Sonographic measurements and appearance of normal kidneys in children, *American Journal of Radiology* 1985, 145:611-616.
18. Taylor, G.A., O'Donnell, R.O. et al. Abdominal injury score: a clinical score for the assignment of risk in children after blunt trauma; *Radiology* 1994, 190:689-694.
19. Dawson-Saunders, B. and Trapp, R.G. *Basic and clinical biostatistics*, Appleton and Lange, 1990, 219-220.



3 9002 08676 0171

HARVEY CUSHING / JOHN HAY WHITNEY
MEDICAL LIBRARY

MANUSCRIPT THESES

Unpublished theses submitted for the Master's and Doctor's degrees and deposited in the Medical Library are to be used only with due regard to the rights of the authors. Bibliographical references may be noted, but passages must not be copied without permission of the authors, and without proper credit being given in subsequent written or published work.

This thesis by _____ has been
used by the following persons, whose signatures attest their acceptance of the
above restrictions.

NAME AND ADDRESS

DATE

